Molecular Microbiology (2017) 104(5), 761–780

doi:10.1111/mmi.13660
First published online 22 March 2017

From substrate specificity to promiscuity: hybrid ABC transporters for osmoprotectants

Laura Teichmann,[1] Chiliang Chen,[1,2] Tamara Hoffmann,[1] Sander H.J. Smits,[3] Lutz Schmitt[3] and Erhard Bremer[1,2]*

[1]*Laboratory for Molecular Microbiology, Department of Biology, Philipps-University Marburg, Karl-von-Frisch Str. 8, Marburg D-35043, Germany.*
[2]*LOEWE-Center for Synthetic Microbiology, Philipps-University Marburg, Hans-Meerweinstr. 6, Marburg D-35043, Germany.*
[3]*Institute of Biochemistry, Heinrich-Heine-University Düsseldorf, Universitätsstr. 1, Düsseldorf D-40225, Germany.*

Summary

The ABC-transporters OpuB and OpuC from *Bacillus subtilis* function as osmoprotectant import systems. Their structural genes have most likely evolved through a duplication event but the two transporters are remarkably different in their substrate profile. OpuB possesses narrow substrate specificity, while OpuC is promiscuous. We assessed the functionality of hybrids between these two ABC-transporters by reciprocally exchanging the coding regions for the OpuBC and OpuCC substrate-binding proteins between the corresponding *opuB* and *opuC* operons. Substantiating the critical role of the binding protein in setting the substrate specificity of ABC transporters, OpuB::OpuCC turned into a promiscuous system, while OpuC::OpuBC now exhibited narrow substrate specificity. Both hybrid transporters possessed a high affinity for their substrates but the transport capacity of the OpuB::OpuCC system was moderate due to the synthesis of only low amounts of the xenogenetic OpuCC protein. Suppressor mutations causing single amino acid substitutions in the GbsR repressor controlling the choline to glycine betaine biosynthesis pathway greatly improved OpuB::OpuCC-mediated compatible solute import through transcriptional up-regulation of the hybrid *opuB::opuCC* operon. Collectively, we demonstrate for the first time that one can synthetically switch the substrate specificity of a given ABC transporter by combining its core components with a xenogenetic ligand-binding protein.

Accepted 27 February, 2017. *For correspondence. E-mail bremer@staff.uni-marburg.de; Tel. (+49) 6421 2821529; Fax (+49) 6421 2828979.

Introduction

ATP binding-cassette (ABC) transporters have an ancient evolutionary history, are found in all kingdoms of life, and both importers and exporters are members of this superfamily (Higgins, 1992; Davidson *et al.*, 2008; Eitinger *et al.*, 2011). They share a common architecture, which, in general, is composed of two subunits of a transmembrane domain (TMD) mediating substrate translocation across the cytoplasmic membrane and two subunits of a nucleotide-binding domain (NBD) that powers substrate translocation through ATP hydrolysis (Patzlaff *et al.*, 2003; Oswald *et al.*, 2006; Oldham *et al.*, 2008; Rees *et al.*, 2009; Beis, 2015; Hopfner, 2016; Locher, 2016).

A large sub-group of the ABC transporter superfamily possesses, in addition to the NBD and TMD core components, an extra-cytoplasmic ligand–binding protein (Davidson *et al.*, 2008; Eitinger *et al.*, 2011; Lewinson and Livnat-Levanon, 2017). These substrate-binding-protein-dependent ABC systems are all importers and probably originated from a common ancestor more than 3 billion years ago (Tam and Saier, 1993; Kuan *et al.*, 1995; Saier, 2000); they are found only in members of the *Bacteria* and *Archaea*. The transport activity of these systems crucially depends on the substrate-binding protein, which plays two important roles for the overall transport process: (i) it scavenges the substrate with high affinity from the surroundings of the cells and delivers it to the TMD core components (Hollenstein *et al.*, 2007; Berntsson *et al.*, 2010; Korkhov *et al.*, 2012b; Oldham *et al.*, 2013; Gouridis *et al.*, 2015; Lewinson and Livnat-Levanon, 2017), and (ii) docking of the binding protein onto the TMDs elicits a conformational signal within the ABC transporter as a whole that leads to the release of the substrate from the binding protein

into the transmembrane translocation route and the subsequent ATP-hydrolysis-dependent extrusion of the substrate into the cytoplasm (Davidson *et al*., 1992; Patzlaff *et al*., 2003; Oswald *et al*., 2006; Daus *et al*., 2007; Shilton, 2008; Grote *et al*., 2009; Khare *et al*., 2009; Orelle *et al*., 2010; Alvarez *et al*., 2015).

In binding-protein-dependent ABC transporters, the core components typically operate in conjunction with a single extra-cytoplasmic substrate-binding protein. This solute receptor is either present as a diffusible protein in the periplasm of Gram-negative bacteria, tethered to the outer face of the cytoplasmic membrane via a lipid anchor in Gram-positive bacteria, covalently attached to the TMD, or anchored to the cytoplasmic membrane by a hydrophobic protein segment in *Archaea* (van der Heide and Poolman, 2002; Albers *et al*., 2004; Davidson *et al*., 2008; Eitinger *et al*., 2011; Gouridis *et al*., 2015; Nguyen and Götz, 2016). However, representatives are also known where multiple binding proteins possessing different affinities or substrate specificities function with the same core components of the ABC transporter (Higgins and Ames, 1981; Oh *et al*., 1994; Leonard *et al*., 1996; Chen *et al*., 2010; Ghimire-Rijal *et al*., 2014), or where multiple binding proteins are fused to the same TMD (van der Heide and Poolman, 2002; Gouridis *et al*., 2015).

All substrate-binding proteins that have been structurally characterized are composed of two rigid lobes connected by either one, two or three flexible linker regions, or a long stiff α-helix (Berntsson *et al*., 2010; Scheepers *et al*., 2016; Lewinson and Livnat-Levanon, 2017). Upon encountering the substrate, the two lobes of the binding protein move towards each other via a hinge-bending movement, and thereby firmly trap the substrate in a deep cleft formed between the two lobes (Mao *et al*., 1982; Quiocho and Ledvina, 1996; Shilton, 2008; Gouridis *et al*., 2015). In depth biochemical and structural studies using the maltose/maltodextrin and vitamin B_{12} ABC transporter from *Escherichia coli*, and the molybdate importer from the archaeon *Archaeoglobus fulgidus* have demonstrated that the cognate substrate-binding protein docks with its two lobes onto either heterodimeric (MalF/MalG), or homo-dimeric (BtuC, or ModB respectively) TMDs (Daus *et al*., 2007; Hollenstein *et al*., 2007; Orelle *et al*., 2008; Grote *et al*., 2009; Korkhov *et al*., 2012a,b; Chen, 2013; Alvarez *et al*., 2015). Through these interactions, the ATPase activity of the corresponding NBD is stimulated by the closed conformation of the binding protein, a process that is stabilized in the presence of the substrate (Orelle *et al*., 2008; Alvarez *et al*., 2015).

The substrate-binding protein is the prime determinant of selectivity in ABC-type import systems (Davidson *et al*., 2008; Berntsson *et al*., 2010; Eitinger *et al*., 2011; Herrou and Crosson, 2013; Scheepers *et al*., 2016). However, a low-affinity substrate-binding site positioned in the TMDs of the maltose/maltodextrin ABC system, a so-called type-I ABC importer (Locher, 2016; Lewinson and Livnat-Levanon, 2017), has been detected genetically and confirmed through crystallographic analysis (Shuman, 1982; Covitz *et al*., 1994; Boos and Shuman, 1998; Oldham *et al*., 2007; 2013; Oldham and Chen, 2011; Chen, 2013). Such a binding site is also present in the TMDs of the arginine/histidine ABC transporter from the thermophile *Thermoanaerobacter tengcongensis* (Yu *et al*., 2015) and probably also in the *myo*-inositol ABC transporter from the fresh-water bacterium *Caulobacter crescentus* (Herrou and Crosson, 2013). This type of internal binding site in the TMDs seems to be absent in type-II ABC importers [e.g., in the BtuCDF transporter for vitamin B_{12} from *E. coli* (Korkhov *et al*., 2012a,b; Locher, 2016; Lewinson and Livnat-Levanon, 2017)].

Binding-protein-dependent ABC transporters can operate against steep concentration gradients, and typically have an affinity for their substrates in the low μM or even nM range (Quiocho and Ledvina, 1996; Boos and Shuman, 1998; Rees *et al*., 2009; Lewinson and Livnat-Levanon, 2017). These properties make them well suited to scavenge their varied substrate(s) from scarce environmental resources and accumulate them inside the cell. They are therefore of great ecophysiological importance for growth and survival of many microorganisms in their natural ecosystems (Davidson *et al*., 2008; Eitinger *et al*., 2011).

ABC transporters feature prominently in the transporter repertoire of the soil bacterium *Bacillus subtilis*. This Gram-positive bacterium possesses 38 of these systems (Quentin *et al*., 1999) and three of them (OpuA, OpuB, OpuC) are involved in the uptake of compatible solutes (Kempf and Bremer, 1995; Kappes *et al*., 1999; Bremer, 2002; Hoffmann and Bremer, 2017). These transporters are members of the type-I subfamily of ABC import systems (Locher, 2016; Lewinson and Livnat-Levanon, 2017). Compatible solutes are stress-relieving compounds and are mostly produced by plants and various microorganisms (Kempf and Bremer, 1998). Their import and high level accumulation aids the *B. subtilis* cells in coping with increases in the external osmolarity by balancing the osmotic gradient across the cytoplasmic membrane (Bremer and Krämer, 2000; Hoffmann and Bremer, 2017). In *B. subtilis* and other microorganisms, the uptake of compatible solutes also serves to offset the detrimental effects of extremes in either low or high temperatures on growth (Holtmann and Bremer, 2004; Hoffmann and Bremer, 2011), a process that is probably dependent on the chemical

chaperon activity of these compounds (Bourot *et al*., 2000; Ignatova and Gierasch, 2006; Street *et al*., 2006).

B. subtilis can derive osmotic and temperature stress protection by taking advantage of a large variety of pre-formed compatible solutes (Hoffmann and Bremer, 2011; 2017). These stress protectants are typically present in low external concentrations in the varied habitats of *B. subtilis* (Welsh, 2000; Bouskill *et al*., 2016; Warren, 2016; Webb *et al*., 2017), and consequently, high-affinity transporters are required to scavenge them. The transport characteristics of the *B. subtilis* Opu transporters with K_m-values in the low μM range meet these requirements (Kappes *et al*., 1996; 1999; Kappes and Bremer, 1998; Bashir *et al*., 2014a,b; Broy *et al*., 2015). The extracellular substrate-binding proteins (OpuAC, OpuBC, OpuCC) of the OpuA, OpuB and OpuC ABC transporters are all lipoproteins (Nguyen and Götz, 2016) anchored via an N-terminal lipid modification to the outer face of the *B. subtilis* cytoplasmic membrane (Kempf and Bremer, 1995; Kempf *et al*., 1997; Kappes *et al*., 1999). Crystal structures of the OpuAC, OpuBC and OpuCC proteins have been reported in complex with various compatible solutes (Horn *et al*., 2006; Smits *et al*., 2008; Du *et al*., 2011; Pittelkow *et al*., 2011).

Among the five osmoprotectant uptake systems (OpuA–OpuE) operating in *B. subtilis* (Hoffmann and Bremer, 2016; 2017), the OpuB and OpuC ABC transporters stand out (Fig. 1). They have most likely evolved through a gene duplication event since the degree of amino acid sequence identity between the components of these systems is extraordinary high and range between 84% for the two ATPases (OpuBA/OpuCA) and 71% for the substrate-binding-proteins (OpuBC/OpuCC) (Kappes *et al*., 1999). Both transporters possess heterodimeric TMDs (OpuBB/OpuBD; OpuCB/OpuCD), with each pair exhibiting an overall sequence identity of 85%; the same value is also found when the TMDs of the OpuB and OpuC transporters are compared with each other (Kappes *et al*., 1999). Despite the close relatedness of the OpuB and OpuC systems, their substrate specificity is strikingly different (Fig. 1). Whereas OpuC imports, with the exception of L-proline and dimethlyglycine (von Blohn *et al*., 1997; Hoffmann *et al*., 2012; Bashir *et al*., 2014b), all of the currently known osmostress protectants for *B. subtilis* (Hoffmann and Bremer, 2017), OpuB serves as a substrate-specific uptake system for choline and glycine betaine aldehyde, the precursor and intermediate in glycine betaine synthesis (Fig. 1), compounds that can also be imported via OpuC (Boch *et al*., 1996; Nau-Wagner *et al*., 2012).

The architecture of the ligand-binding sites of the OpuBC and OpuCC proteins is very similar (Du *et al*., 2011; Pittelkow *et al*., 2011) and allows to a certain extent the flexible positioning of the positively charged head-groups of the ligands through cation–π interactions (Mahadevi and Sastry, 2013) within an architectural identical aromatic cage formed by four Tyr residues (Du *et al*., 2011; Pittelkow *et al*., 2011; Bashir *et al*., 2014a,b; Broy *et al*., 2015). However, small differences between the residues coordinating the "tail" of the various ligands significantly influences substrate specificity, in particular those that are involved in the closing of the two lobes of the binding protein when it traps the ligand (Du *et al*., 2011; Pittelkow *et al*., 2011).

The close structural relationship of the components of the OpuB and OpuC systems on the one hand, and their strikingly different substrate profile on the other hand (Fig. 1) raise intriguing questions about the molecular underpinnings governing the substrate specificity of the entire ABC transporter. Here we report the successful construction of functional hybrids between the OpuB and OpuC transporters in which the corresponding ligand-binding proteins (OpuBC and OpuCC) were reciprocally exchanged. In these hybrid transporters, the ligand-binding protein dictates the overall substrate profile of the synthetic transporter in accordance with the Opu ABC system from which it was originally derived. This is the first example of a switch in substrate specificity of a given ABC transporter by combining its core components with a xenogenetic substrate-binding protein, data that re-enforce the central role played by the extra-cytoplasmic ligand-binding protein for the overall functioning of these importer systems. They also pose intriguing questions about the evolution of the *B. subtilis* OpuB and OpuC transporters.

Results

Design and functional assessment of the chassis strains

To functionally study the OpuB and OpuC ABC transporters and their mutant derivatives, we constructed a chassis strain (TMB118) (Supporting Information Table S1) that lacked, with the exception of the L-proline osmolyte transporter OpuE (von Blohn *et al*., 1997; Hoffmann *et al*., 2012), all osmostress protectant uptake systems (OpuA, OpuB, OpuC, OpuD) operating in *B. subtilis* (Hoffmann and Bremer, 2016; 2017) (Fig. 1). We then separately introduced intact *opuB* and *opuC* operons into the chassis strain by positioning them ectopically in single copy into the *B. subtilis* genome at the dispensable *amyE* gene. This yielded strains CCB2 (*amyE::opuB*$^+$) and CCB3 (*amyE::opuC*$^+$) respectively. In the chassis strain TMB118, the chromosomal *opuB* and *opuC* operons are completely deleted (Supporting Information Table S1), and consequently no

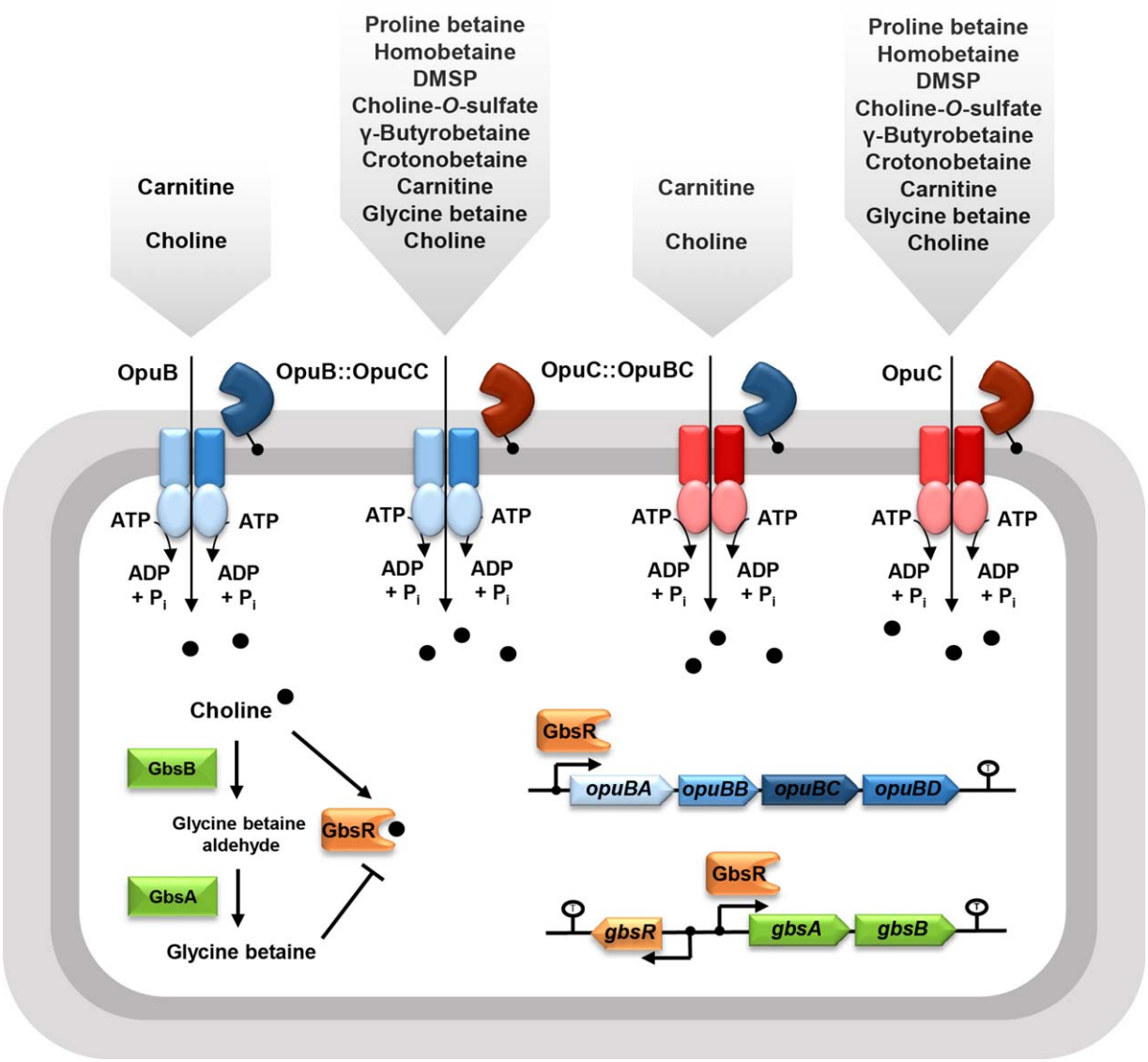

Fig. 1. Substrate specificities of the Opu osmoprotectant uptake systems OpuB and OpuC and the hybrid OpuB::OpuCC and OpuC::OpuBC transport system derived from them. The wild-type OpuB and OpuC ABC transporters and the hybrid systems are depicted along with their substrate profile. The osmoadaptive choline-to-glycine betaine biosynthetic pathway and its regulation through the choline-sensing regulator GbsR is also shown. Black dots represent choline, which serves both as the precursor for the GbsBA-mediated synthesis of glycine betaine and as the inducer for the GbsR repressor. The newly formed glycine betaine re-establishes, in a not fully understood regulatory circuit, GbsR-mediated repression of *gbsAB* and *opuB* expression (Boch *et al*., 1996; Nau-Wagner *et al*., 2012).

recombination can take place between the natural *opu* loci and the synthetic *amyE::opuB* and *amyE::opuC* constructs. Furthermore, since the *opuB* and *opuC* gene clusters inserted in *amyE* are expressed from their natural osmostress-responsive promoters (Kappes *et al*., 1999), no multi-copy effects can potentially complicate the interpretation of the obtained data.

As expected, and in contrast to its parent strain JH642, the chassis strain TMB118 could no longer be protected from high-osmolarity-induced stress by any of the nine compatible solutes that we used in our study (Fig. 2) and that can otherwise be imported either via OpuB or OpuC (Fig. 1). In contrast, the pattern of osmostress protection of strains CCB2 (*amyE::opuB*$^+$) and CCB3 (*amyE::opuC*$^+$) (Fig. 2) by compatible solutes matched that found previously in *B. subtilis* strains carrying either intact *opuB* or *opuC* operons at their natural genomic loci (Hoffmann and Bremer, 2017). There was one notable exception: in contrast to a previous report (Kappes and Bremer, 1998), L-carnitine was not only imported via OpuC but was also taken up via OpuB (Fig. 2). However, osmostress protection by L-carnitine is not a peculiarity of the recombinant CCB2 (*amyE::opuB*$^+$) strain, but was also found upon re-assessment of a strain

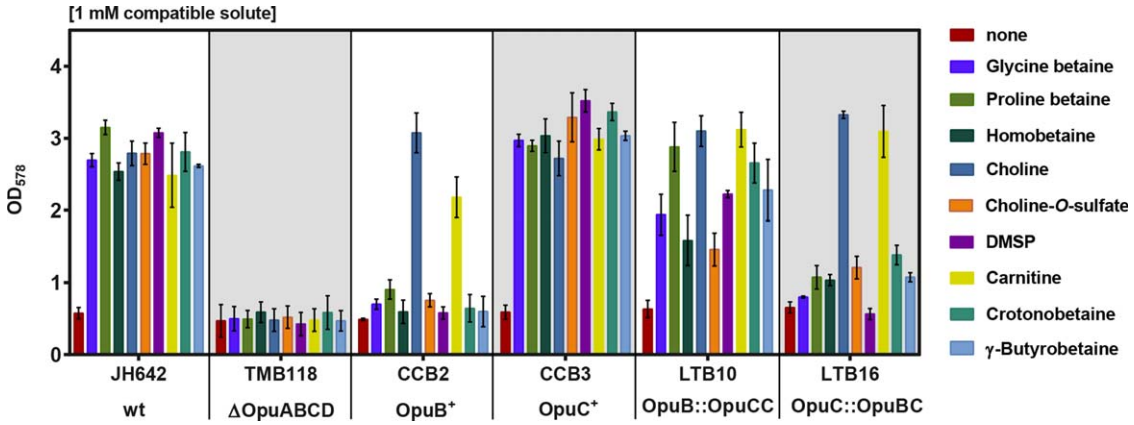

Fig. 2. Osmostress protection under high-salinity growth conditions and import of various compatible solutes via the OpuB, OpuC, OpuB::OpuCC and OpuC::OpuBC ABC transport systems. Cells of *B. subtilis* strains were grown in SMM containing 1.2 M NaCl in the absence or presence of 1 mM (final concentration) of various compatible solutes. The growth yield of the cultures was determined by measuring their OD_{578} after 16 h of incubation at 37°C, except for strain LTB10 which was cultivated for 17 h. The shown values represent data from two independent biological replicates. In strains CCB2 and CCB3 only the indicated Opu transporters are active and this is marked by a plus (+) superscript.

expressing the *opuB* operon at its natural location in the *B. subtilis* genome (Supporting Information Fig. S1).

OpuB and OpuC transporters lacking their solute receptor protein are nonfunctional

After we had re-confirmed that OpuB was a narrow substrate-specific transporter and that OpuC was a highly promiscuous system (Fig. 2) (Hoffmann and Bremer, 2011; 2017), we ensured that the extracellular ligand-binding proteins (OpuBC, OpuCC) (Fig. 1) were required for the functionality of these two ABC transporters. To this end, we constructed derivatives of the *opuB* and *opuC* operons (Kappes *et al.*, 1999) in which the coding regions (*opuBC* and *opuCC*) for the corresponding OpuBC and OpuCC ligand-binding proteins were precisely deleted (Supporting Information Fig. S2). The integration of the corresponding mutant *opuB* and *opuC* gene clusters into TMB118 yielded strains (LTB15 and LTB14) that could, as expected, no longer be protected by any of the tested compatible solutes (Supporting Information Fig. S3). Hence, as observed in previous studies with mutants of the *E. coli* maltose ABC transporter lacking the periplasmic MalE substrate-binding protein (Covitz *et al.*, 1994; Boos and Shuman, 1998), the *B. subtilis* OpuB and OpuC ABC transporters strictly rely for their functioning on the extracellular OpuBC and OpuCC substrate-binding proteins.

Hybrid OpuB::OpuCC and OpuC::OpuBC transporters are functional

In the next step of our functional analysis of the OpuB and OpuC ABC transporters, we substituted the coding region for the OpuBC ligand-binding protein with that of its OpuCC counterpart [OpuB::OpuCC] and we also constructed the reciprocal transport system [OpuC::-OpuBC]. Western blot analysis of cell extracts prepared from the resulting strains LTB10 (*amyE::opuB*::*opuCC*$^{+}$) and LTB16 (*amyE::opuC*::*opuBC*$^{+}$) with polyclonal antisera recognizing the OpuBC and OpuCC proteins (Kappes *et al.*, 1999) demonstrated that the expression of the synthetic operons led to the production of hybrid ABC transporters containing the "xenogenetic" ligand-binding protein (Supporting Information Fig. S4).

We then tested the substrate profile of the hybrid OpuB::OpuCC and OpuC::OpuBC transporters in osmostress protection growth assays in a minimal medium (SMM) containing 1.2 M NaCl. We observed a striking switch in substrate specificity of the synthetic ABC transporters (Fig. 2). Integration of the OpuCC ligand-binding protein into the OpuBC-gutted OpuB system yielded a transporter with broad substrate specificity; its substrate profile matched that of the intact OpuC transporter. Conversely, the hybrid OpuC::OpuBC system now was converted into a transporter that afforded only efficient osmostress protection by choline and carnitine, while at the same time the other tested compatible solutes provided only a low degree of stress protection (Fig. 2).

Kinetic parameters of the hybrid OpuB::OpuCC and OpuC::OpuBC transporters

To further characterize the hybrid OpuB::OpuCC and OpuC::OpuBC ABC transporters, we assessed their kinetic parameters for choline, glycine betaine and carnitine uptake using radiolabeled substrates and compared them

Table 1. The effect of xenogenetic substrate-binding proteins on the kinetic properties of hybrid OpuC::OpuBC and OpuB::OpuCC ABC transporters.

Transporter	Substrate	V_{max} (nmol min^{-1} mg^{-1})	K_m (μM)
OpuC	Glycine betaine	100 ± 5	5 ± 1
	Choline	81 ± 3	27 ± 4
	Carnitine	94 ± 5	8 ± 2
OpuB::OpuCC	Glycine betaine	20 ± 1	6 ± 1
	Choline	14 ± 1	26 ± 3
	Carnitine	14 ± 0	4 ± 1
OpuB	Choline	67 ± 2	3 ± 1
	Carnitine	126 ± 5	1139 ± 127
OpuC::OpuBC	Choline	124 ± 3	6 ± 1
	Carnitine	306 ± 14	3708 ± 414

Cells of *B. subtilis* strains were propagated at 37°C in SMM containing 0.4 M NaCl to early-exponential growth phase (OD_{578} of about 0.3) and were then used for uptake studies with radiolabeled glycine betaine, choline and carnitine. Each of the transport assays was conducted with two independently grown cultures, and the reported errors represent the corresponding standard deviations.

with the authentic OpuB and OpuC transporters. For these experiments, we grew the LTB10 (*amyE::opuB*::*opuCC*$^+$) and LTB16 (*amyE::opuC*::*opuBC*$^+$) strains and their *opuB*$^+$ (strain CCB2) and *opuC*$^+$ (strain CCB3) counterparts in a chemically defined medium (SMM) containing 0.4 M NaCl to osmotically induce the expression of the various *opu* gene clusters (Kappes *et al*., 1999).

The native OpuC system recognized choline, glycine betaine and carnitine with high affinity (K_m) and it possessed a substantial capacity (V_{max}) for each of these three substrates (Table 1; Supporting Information Fig. S5). The OpuB::OpuCC transporter recognized the same substrates with similar high affinity but its capacity was notably reduced in comparison with the authentic OpuC transporter (Table 1). As reported previously (Kappes and Bremer, 1998), the OpuB transporter exhibited a high affinity and substantial transport capacity for choline. However, for its newly detected substrate carnitine (Fig. 2), it displayed a rather low affinity, yet it possessed, quite surprisingly, a high transport capacity for this substrate (Table 1). At this point, we also cannot provide a rational explanation why the K_m of the OpuB transporter for carnitine is so high (more than 1 mM); yet the V_{max} for this substrate is twofold higher than that for choline (Table 1). The hybrid OpuC::OpuBC transporter displayed affinities for choline and carnitine similar to that of the native OpuB transporter but its capacity for these two substrates was notably increased (Table 1). Changes in V_{max} can result from different production levels of subunits of the ABC transporter, or from altered interaction between the xenogenetic substrate binding protein with the heterologous TMDs. The uptake of carnitine via OpuB and the OpuC::OpuBC hybrid transporter (Table 1) requires further study, in particular in view of the fact that the uptake of carnitine via OpuB was previously missed (Kappes and Bremer, 1998).

The hybrid OpuB::OpuCC transporter is inefficient to relieve osmotic stress

For the further analysis of the hybrid ABC transporters we focused on the OpuB system with the transplanted OpuCC ligand-binding protein since it exhibited novel properties and a broad substrate profile (Fig. 1). Osmostress protection growth assays (Fig. 2) were carried out in high-salinity (1.2 M NaCl) minimal media in which the various compatible solutes were supplied to the *B. subtilis* cells at a final concentration of 1 mM. The ineffectiveness of the hybrid OpuB::OpuCC transporter to restore growth under osmotically unfavorable conditions became visible in assays, when we lowered the concentration of the osmostress protectants by fivefold down to 0.2 mM. Such a low concentration of the compatible solutes still allowed effective osmostress protection for a strain (CCB3) producing exclusively the wild-type OpuC transporter, whereas the operation of the OpuB::OpuCC hybrid transporter could only provide marginal stress protection to cells of strain LTB10 challenged by high osmolarity (Fig. 3). In these growth assays (see also Fig. 2) we observed minor differences in the effectiveness of some compatible solutes (e.g., choline-*O*-sulfate, DMSP) to protect the cells from the detrimental effects of high salinity. While we do not know the precise reasons for this phenomenon, it might be related to different physico-chemical properties of various compatible solutes (Street *et al*., 2006), as it is known that not all representatives of these organic compounds are created equal with respect to stress protection of *B. subtilis* (Hoffmann and Bremer, 2011; Bashir *et al*., 2014a, 2014b; Broy *et al*., 2015).

To obtain further insights into the ineffectiveness of the hybrid OpuB::OpuCC transporter at a low supply of the osmostress protectants we probed the amount of the OpuCC ligand-binding protein in a Western blot experiment. We observed that the xenogenetic OpuCC ligand-binding protein paired with the remaining OpuB transporter components was present at a substantially lower amount in comparison with the native OpuC transporter (Fig. 4A). This finding suggests that the limiting factor for the relative ineffectiveness of the hybrid OpuB::OpuCC transporter to provide osmostress protection was likely due to the low level of the xenogenetic OpuCC ligand-binding protein.

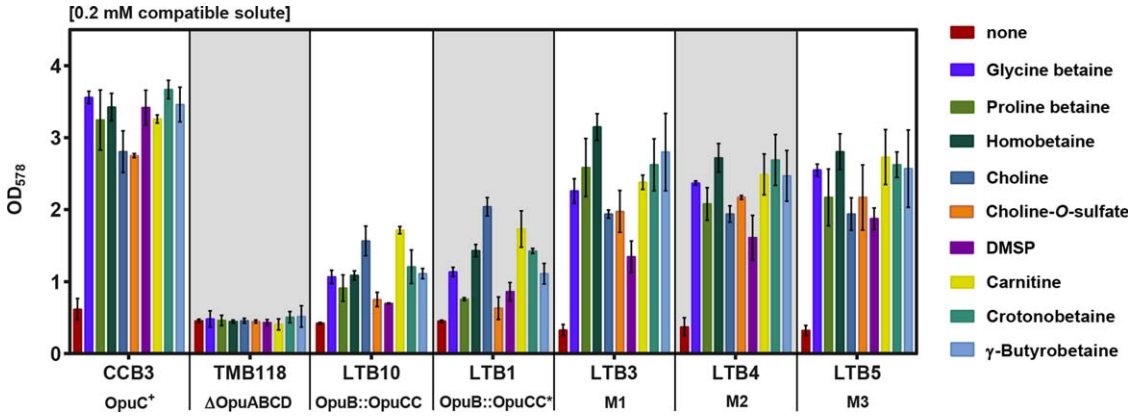

Fig. 3. Osmostress protection of *B. subtilis* strains under growth conditions with a low concentration of compatible solutes. Strains possessing different Opu transporters were grown in SMM containing 1.2 M NaCl in the absence or presence of 0.2 mM (final concentration) of the various compatible solutes. The growth yield of the cultures was determined by measuring their OD_{578} after 17 h of incubation at 37°C. Strain LTB1, from which the suppressor mutant strains LTB3, LTB4 and LTB5 are derived, carries the *gbsR*$^{+}$ wild-type gene. The suppressor strains carry the M1 (Gly^{39}/Glu; strain LTB3), M2 (Thr^{79}/Ala; strain LTB4) and M3 (Arg^{85}/Ser; strain LTB5) *gbsR* mutant alleles. The shown values represent data from two independent biological replicates and the reported errors represent the corresponding standard deviation. In strain CCB3 only the OpuC transporter is active and this is marked by a plus (+) superscript. In strain LTB1 the OpuCC protein of the hybrid OpuB::OpuCC* transporter carries a Met^{211} to Ile substitution (see Fig. S7) and this fact is indicated by a star (*).

Isolation and functional characterization of suppressor mutants improving the efficiency of the hybrid OpuB::OpuCC system

Prompted by our finding that the transport capacity (V_{max}) of the hybrid OpuB::OpuCC transporter was low (Table 1) and that it functioned only ineffectively at low substrate concentration in osmostress protection assays (Fig. 4B), we devised a genetic screen that selected for strains that show enhanced growth at high salinity in the presence of low concentrations of an osmostress protectant. We observed that the OpuB::OpuCC strain LTB1 plated far less efficiently on SMM agar plates containing 1.1 M NaCl and only 50 μM of the osmostress protectant glycine betaine than a strain possessing an authentic OpuC system. However, faster-growing colonies appeared on these plates with an approximate frequency of 5.3×10^{-7} (Fig. 4C).

We chose three independently isolated suppressor mutant strains [LTB3 (M1), LTB4 (M2) and LTB5 (M3)] for further analysis. First, we observed that the suppressor mutants now plated in spot growth assay with increased efficiency on the agar plates used for the original selection of the mutants (Fig. 4D). Second, osmostress protection growth assays in liquid media that contained low concentrations (0.2 mM) of osmostress protectants revealed that each of the suppressor strains could efficiently use the full spectrum of the provided compatible solutes (Fig. 3). Finally, and most tellingly, was our finding that the amount of the OpuCC binding protein detected in a Western blot of cell extracts prepared from the LTB3 (M1), LTB4 (M2) and LTB5 (M3) suppressor strains was strongly increased compared with the amount produced by the OpuB::OpuCC parent strain LTB1. The level of OpuCC in the three suppressor mutants even exceeded that produced by an authentic OpuC^{+} strain (Fig. 4A).

We then determined the kinetic parameters of the OpuB::OpuCC transporter in the three suppressor strains and compared them with those of the parent for one of the substrate, glycine betaine. In transport assays with radiolabeled glycine betaine, we observed that the LTB3 (M1), LTB4 (M2) and LTB5 (M3) suppressor strains had retained an affinity (K_m) for their substrates similar to the parental OpuB::OpuCC strain LTB1. However, their transport capacity (V_{max}) was now substantially improved (Table 2; Supporting Information Fig. S6).

Prior to the isolation of the suppressor mutants, we had overlooked in our DNA-sequence analysis of the hybrid *opuB*::*opuCC* gene cluster present in strain LTB1 that the *opuCC* gene had inadvertently picked up a point mutation [ATG to ATA] during the construction of the hybrid operon. The resulting amino acid substitution [Met^{211}/Ile] is located at a considerable distance from the OpuCC ligand-binding site (Supporting Information Fig. S7) and is also not present in an area of OpuCC predicted to interact with the TMDs (Supporting Information Fig. S8A and B). We reconstructed the *opuCC* wild-type sequence in the hybrid *opuB*::*opuCC* operon through site-directed mutagenesis. The resulting strain LTB10 exhibited the same growth pattern as strain LTB1 in high-salinity media containing low concentrations of compatible solutes (Fig. 3). Consequently, the *opuB*::*opuCC** (Met^{211}/Ile) variant was immaterial for the

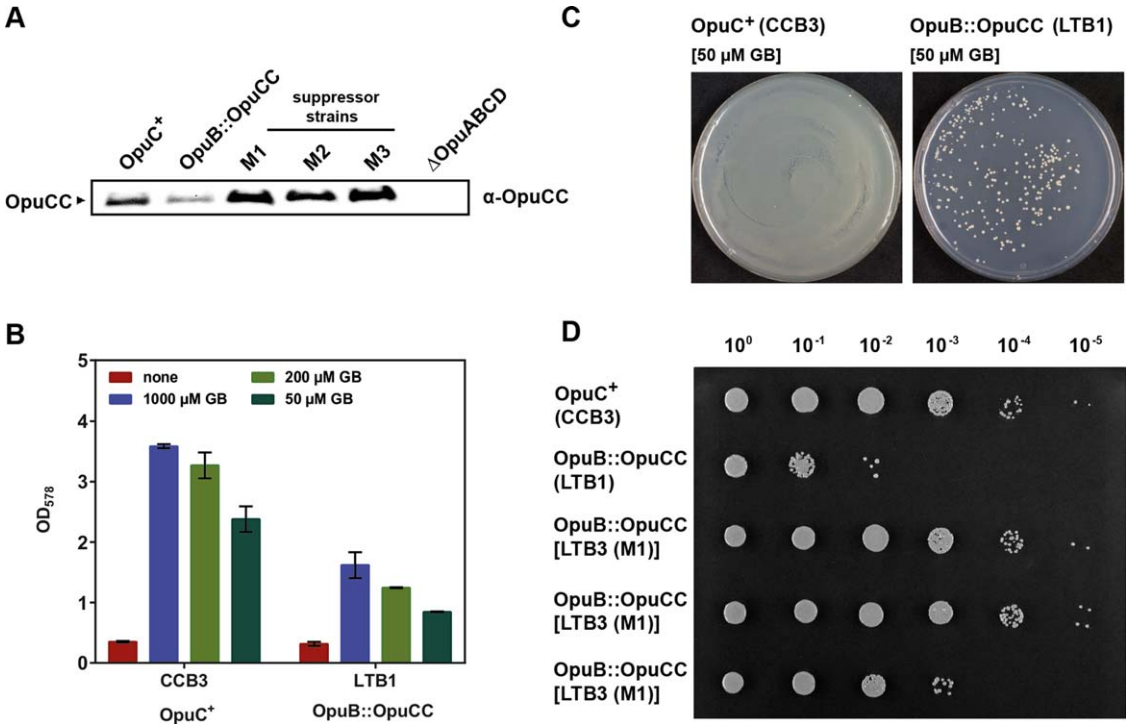

Fig. 4. A. Detection of the OpuCC ligand-binding protein by immunoblot analysis and isolation of suppressor mutants. Proteins of total cell lysates of *B. subtilis* strains grown in SMM with 1.2 M NaCl were separated by SDS-PAGE followed by Western blot analysis. Sample normalization was achieved by adjusting the cell suspensions to the same OD_{578}. Proteins transferred to the blotting membrane were probed with a polyclonal antiserum raised against OpuCC (Kappes *et al*., 1999).
B. The OpuC$^+$ strain CCB3 and its OpuB::OpuCC derivative LTB1 were grown in SMM containing 1.2 M NaCl and the indicated concentrations of the compatible solute glycine betaine. The growth yield of the cultures was determined by measuring their OD_{578} after 17 h of incubation at 37°C. The shown values represent data from two independent biological replicates and the reported errors represent the corresponding standard deviation.
C. The OpuC$^+$ strain CCB3 and its OpuB::OpuCC derivative LTB1 were grown in SMM containing 0.4 M NaCl until the cultures reached an OD_{578} of about 2. 0.1-ml aliquots of 10^{-1} dilutions of these cultures (prepared in the growth medium) were plated on SMM agar plates containing 1.1 M NaCl and 50 μM glycine betaine. The agar plates were incubated for five days at 37°C.
D. Spot growth assays were conducted with the *B. subtilis gbsR*$^+$ *opuB*::*opuCC** LTB1 parent strain and its three *gbsR* suppressor mutant (M1–M3) derivatives [strains LTB3 (*gbsR*-Gly^{39}/Glu), LTB4 (*gbsR*-Thr^{79}/Ala) and LTB5 (*gbsR*-Arg^{85}/Ser)] on SMM agar plates containing 1.1 M NaCl and 50 μM glycine betaine. For the adaptation of the strains the to high-salt growth conditions, the cultures were pre-grown in SMM containing 0.4 M NaCl. After reaching late exponential phase (OD_{578} of 2), 5 μl of serial dilutions prepared from the cell suspensions with the growth medium were spotted onto agar plates, which were then incubated at 37°C for three days.

suppressor selection that we carried out with strain LTB1 (Fig. 4C and D).

De-repression of transcription of the opuB::opuCC *operon is responsible for enhanced growth of the suppressor mutants at high salinity*

The molecular underpinnings for the increased production of the xenogenetic OpuCC binding protein by the LTB3 (M1), LTB4 (M2) and LTB5 (M3) suppressor strains (Fig. 4A) could lie either within the hybrid *opuB::opuCC* operon itself, in *cis*-acting regulatory sequences controlling its transcription (Kappes *et al*., 1999; Lee *et al*., 2013; Winkelman *et al*., 2013), or in the *trans*-acting regulatory gene *gbsR* that encodes a repressor (GbsR) for the *opuB* operon (Fig. 1) (Nau-Wagner *et al*., 2012). We sequenced the *opuB*::*opuCC* and *gbsR* loci of the suppressor strains LTB3 (M1), LTB4 (M2) and LTB5 (M3) and compared these DNA sequences with those present in the parent strain LTB1. No changes were detected in the *opuB*::*opuCC* operons of the M1, M2 and M3 suppressor mutants, but each of them harbored point mutations in *gbsR* that led to single amino acid substitutions at either position 39 [Gly/Glu] (M1), 79 [Thr/Ala] (M2) or 85 [Arg/Ser] (M3) in the 180 amino acid-comprising GbsR regulatory protein (Nau-Wagner *et al*., 2012) (Fig. 5A).

Based on the observed increase in the OpuCC protein levels (Fig. 4A), we hypothesized that the M1, M2 and M3 suppressor mutations affect the strength of GbsR-mediated repression of *opuB::opuCC* transcription in strains LTB3, LTB4 and LTB5 in the absence of the GbsR inducer choline (Nau-Wagner *et al*., 2012). If this assumption is correct, then these mutations should also

Table 2. Kinetic parameters for the uptake of glycine betaine via the hybrid ABC transporter OpuB::OpuCC expressed in the parent strain LTB1 and its three suppressor derivatives.

Transporter	*gbsR* allele	V_{max} (nmol min^{-1} mg^{-1})	K_m (μM)
[a]OpuB::OpuCC*	*gbsR*$^+$	16 ± 1	9 ± 1
[a]OpuB::OpuCC*	*gbsR*-Gly^{39}/Glu (M1)	92 ± 5	12 ± 2
[a]OpuB::OpuCC*	*gbsR*-Thr^{79}/Ala (M2)	99 ± 6	15 ± 3
[a]OpuB::OpuCC*	*gbsR*-Arg^{85}/Ser (M3)	95 ± 4	14 ± 2

Cells of *B. subtilis* strains were propagated at 37°C in SMM containing 0.4 M NaCl to early-exponential growth phase (OD_{578} of about 0.3) and were then used for uptake studies with radiolabeled glycine betaine. Each of the transport assays was conducted with two independently grown cultures, and the reported errors represent the corresponding standard deviations.
a. The OpuB::OpuCC* transporter present in strain LTB1, and its M1, M2 and M3 suppressor derivatives with mutations in *gbsR*, carries a Met^{211} to Ile amino acid substitution in the mature OpuCC protein (see Supporting Information Fig. S7); however it does not affect the substrate profile of this transporter in comparison with an OpuB::OpuCC system (present in strain LTB10) possessing the wild-type OpuCC protein (see the growth data for these two strains in Fig. 3).

affect the expression of the *gbsAB* glycine betaine biosynthetic gene cluster (Fig. 1) as it is also under GbsR control (Boch *et al*., 1996; Nau-Wagner *et al*., 2012). We tested the influence of the three recovered *gbsR* mutant alleles on the expression levels and regulatory profiles of the *opuB* and *gbsAB* operons by genetically combining them with single-copy *opuB-treA* and *gbsAB-treA* operon fusions that report the activity of the corresponding GbsR-controlled promoters. The transcription of the *opuB* operon is not only controlled by GbsR but is also induced by increases in the external osmolarity, regulatory inputs into the transcriptional profile of *opuB* that operate independently from each other (Kappes *et al*., 1999; Nau-Wagner *et al*., 2012). The *opuB-treA* reporter fusion faithfully reflected this regulatory pattern, both in a *gbsR* wild-type and in a *gbsR::neo*^{R} deletion mutant genetic background (Fig. 5B). The three suppressor strains altered the level but not the pattern of *opuB-treA* expression. In each of the fusion strains harboring the *gbsR* suppressor mutations, the basal level of *opuB-treA* expression was strongly increased and substantially exceeded the one observed in *gbsR* wild-type cells grown at increased salinity (Fig. 5B). Despite the substantially increased basal level of *opuB-treA* expression, the M1, M2 and M3 *gbsR* mutations still allowed osmotic induction of the *opuB-treA* reporter fusion (Fig. 5B).

Transcription of the *gbsAB* genes is strongly enhanced in a GbsR-dependent fashion by the presence of the inducer choline in the growth medium (Nau-Wagner *et al*., 2012). When the influence of the M1, M2 and M3 *gbsR* suppressor mutants on the expression of a *gbsA-treA* reporter fusion was tested, each of them led to a substantial increase in the basal level of transcription in the absence of the inducer (Fig. 5C). In this test, the *gbsR*-M1 point mutant behaved liked a *gbsR::neo*^{R} deletion mutant in that it led to a high level of expression and non-responsiveness to the inducer choline, while the M2 and M3 *gbsR* mutants proved to be still responsive to the inducer choline (Fig. 5C).

A homology model of the choline-responsive GbsR protein from *B. subtilis* has previously been constructed *in silico* (Nau-Wagner *et al*., 2012) and is based on a crystal structure of a protein (Mj223) of unknown function from the thermophilic methanogenic archaeon *Methanococcus jannaschii* (PDB code 1KU9) (Ray *et al*., 2003). Both proteins belong to the widely distributed MarR superfamily of transcriptional regulators (Wilkinson and Grove, 2006). The Mj223 and GbsR proteins are functional dimers, and the *in silico* model of a GbsR monomer is shown in Fig. 5A. GbsR possesses a carboxy-terminal dimerization domain that is connected with a flexible linker region to the amino-terminal DNA-reading head, which contains a helix-turn-helix (HTH) winged helix DNA-binding motif. An aromatic cage like structure resembling that of choline substrate-binding proteins of ABC transporters (Oswald *et al*., 2008; Du *et al*., 2011; Pittelkow *et al*., 2011) is present at the intersection between the carboxy- and amino-terminal domains that putatively constitute the ligand-binding site for the GbsR inducer choline (Nau-Wagner *et al*., 2012). The M1 suppressor mutation [Gly^{39}/Glu] is present in the DNA-reading head and is located in a short helix that is packed against the helix-turn-helix DNA-binding region (Fig. 5A). The M2 [Thr^{79}/Ala] and M3 [Arg^{85}/Ser] single amino acid substitutions are located in the flexible linker region (Fig. 5A) thought to transmit the inducer-mediated re-orientation of both the dimerization and DNA-binding domains when GbsR detaches from its operator sequence in the *gbsAB* and *opuB* regulatory regions (Ray *et al*., 2003; Nau-Wagner *et al*., 2012). Collectively, these data on the altered transcriptional control of the *opuB* and *gbsAB* gene clusters in the *gbsR* suppressor isolates readily allow an understanding why the amount of the OpuCC binding protein is substantially increased in the LTB3 (M1), LTB4 (M2) and

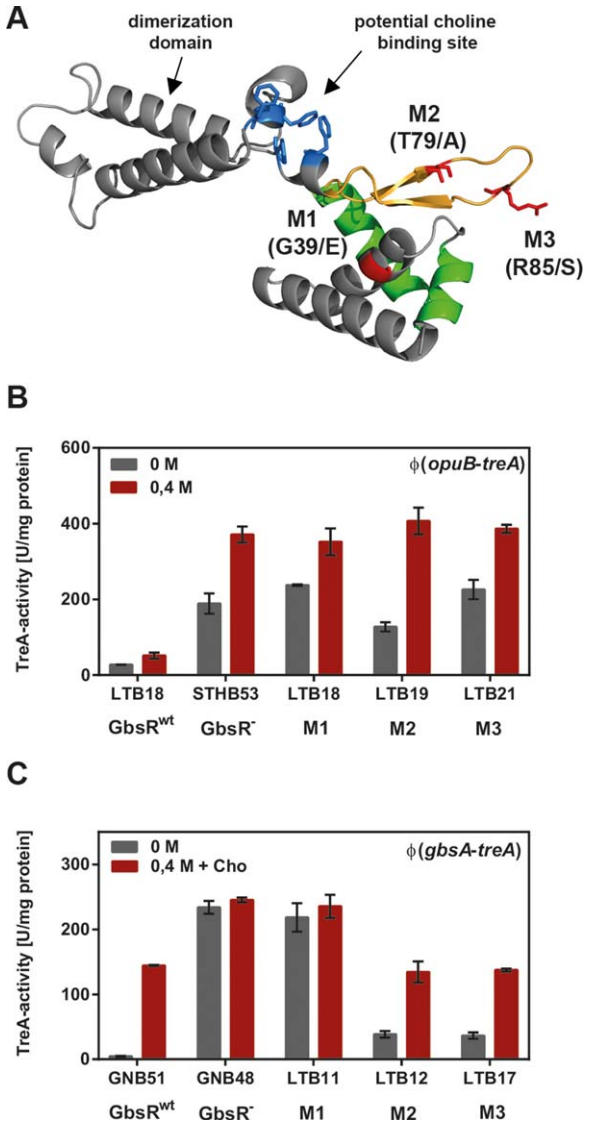

Fig. 5. GbsR-dependent regulation of *opuB* and *gbsAB* expression.
A. Predicted structure of the *B. subtilis* GbsR monomer derived by *in silico* modeling using the PDB entry 1KU9 of the *M. jannaschii* Mj223 protein as the template (Ray *et al.*, 2003; Nau-Wagner *et al.*, 2012). The predicted helix-turn-helix winged helix DNA-binding motif is shown in green, the four Phe residues predicted to form part of the binding pocket for the inducer choline are shown in blue, and the flexible linker region, connecting the amino-terminal DNA-reading head with the carboxy-terminal dimerization domain, is shown in yellow. Onto this predicted three-dimensional GbsR structure, we projected the positions of the amino acid substitutions that have occurred in the M1 (G^{39}/E), M2 (T^{79}/A) and M3 (R^{85}/S) *gbsR* suppressor mutant strains.
B. Cells carrying a chromosomal *opuB-treA* reporter gene fusion and the wild-type *gbsR* gene ($GbsR^{wt}$), a *gbsR*::*neo*^{R} gene disruption ($GbsR^-$), or the M1, M2, M3 *gbsR* suppressor alleles were grown at 37°C either in SMM (gray bars) or in SMM with 0.4 M NaCl (red bars) to an OD_{578} of 1, and aliquots of the cells were then assayed for TreA reporter enzyme activity.
C. Strains with either an intact *gbsR* gene ($GbsR^{wt}$), a *gbsR*::*neo*^{R} gene disruption mutation ($GbsR^-$), or mutant *gbsR* alleles (M1, M2, M3 suppressor strains) that carried a chromosomal *gbsA-treA* reporter gene fusion were grown at 37°C in SMM to early log phase (OD_{578} of 0.25). Aliquots were then assayed for TreA reporter enzyme activity (non-induced, gray bars). At this time point, 1 mM choline and 0.4 M NaCl were added to the cultures to trigger osmotically stimulated import of the GbsR-inducer choline by cells (Nau-Wagner *et al.*, 2012); after 90 min of further incubation the cultures were harvested for TreA enzyme activity assay (induced, red bars).

LTB5 (M3) mutant strains producing the hybrid OpuB::OpuCC transporter (Fig. 4A).

Although we have not identified the precise molecular underpinnings for the reduced synthesis of the xenogenetic OpuCC protein in the original OpuB::OpuCC strain LTB1 (Fig. 4A), we note in this context that a tiling array study of environmentally or nutritionally challenged *B. subtilis* cells revealed the synthesis of a SigB-dependent long anti-sense RNA that originates in the last gene of the *opuB* operon (*opuBA-opuBB-opuBC-opuBD*) and extends into the first gene of this gene cluster (Nicolas *et al.*, 2012). This anti-sense RNA can basepair perfectly with the authentic *opuB* mRNA. The regulatory and physiological role of this *opuB* anti-sense RNA is not known but it seems possible that the foreign *opuCC* segment in the synthetic *opuBA-opuBB-opuCC-opuBD* gene cluster could lead to a destabilization of the corresponding mRNA because its pairing with the *opuB* anti-sense RNA is now impaired. Indeed, the degree of nucleotide sequence identity of the *opuBC* and *opuCC* coding regions is only 70%.

Discussion

Binding-protein-dependent ABC transporters essentially all possess the same set of subunits (Davidson *et al.*, 2008; Oldham *et al.*, 2008; Rees *et al.*, 2009; Eitinger *et al.*, 2011; Beis, 2015; Locher, 2016; Lewinson and Livnat-Levanon, 2017) and are thus in their core modular systems. However, to the best of our knowledge, construction of functional hybrids has only been reported in a single case when the ATPases of the ABC transporters for *sn*-glycerol-3-phosphate (Ugp) and maltose (Mal) from *E. coli* were reciprocally exchanged (Hekstra and Tommassen, 1993; Wuttge *et al.*, 2012). The ATPases of binding-protein dependent ABC systems are the most conserved subunits of these types of transporters (Davidson *et al.*, 2008; Eitinger *et al.*, 2011) and functionally exchangeability seemed therefore likely. However, the Ugp/Mal hybrids were less efficient in their transport capabilities and less stable than the corresponding wild-type transporters. These data indicate that evolution has intimately shaped the protein:protein

interactions between the components of a given ABC transporter so that their subunits cannot be readily exchanged with those of other ABC systems. Indeed, the genes for the substrate-binding protein, for the TMD(s) and for the NBD of a given ABC system mostly co-evolve in the same operon, and in the course of evolution there is little evidence for a mix and match of individual components between different ABC transporters (Kuan *et al*., 1995).

Despite these apparent constraints, we report here the first example of a successful construction of synthetic ABC transporters that contained xenogenetic binding proteins. Using the sequence related OpuB and OpuC osmostress protectant uptake systems from *B. subtilis* as model systems (Kappes *et al*., 1999; Hoffmann and Bremer, 2017) (Fig. 1), we were able to generate functional hybrid ABC transporters through the exchange of the genes for the corresponding ligand-binding proteins, OpuBC and OpuCC. These hybrid transporters possessed substrate profiles that were dictated by the substrate spectrum of the Opu system from which the binding protein was originally derived (Figs 2 and 3). Collectively, these data strongly reinforce the view that the ligand-binding properties of the extracellular substrate-binding proteins are the prime determinant for the overall specificity and affinity of a given ABC transporter (Boos and Shuman, 1998; Davidson *et al*., 2008; Eitinger *et al*., 2011).

It is highly likely that our ability to construct functional hybrids of the OpuB and OpuC systems was aided through their evolutionary history as these transporters probably originated from a gene duplication event (Kappes *et al*., 1999). Judging from the transporter characteristics, substrate profile and degree of osmostress protection afforded by the OpuC::OpuBC and OpuB::OpuCC hybrid systems (Tables 1 and 2, Fig. 3), the xenogenetic binding proteins were able to dock onto the TMDs of the heterologous transporter but these interactions might not be perfect. Inspired by the crystal structure of the type-I molybdate transporter (ModBC) from the archaeon *A. fulgidus* in complex with its substrate-binding protein (ModA) (PDB accession number 2ONK) (Hollenstein *et al*., 2007), our modeling studies suggest that three regions of the OpuBC and OpuCC proteins (Supporting Information Fig. S8A) might interact with the cognate TMDs of the OpuB (OpuBB/OpuBD) and OpuC (OpuCB/OpuCD) transport systems. The spatial organization and charge distribution of these three regions is very similar in OpuBC and OpuCC (Supporting Information Fig. S8B). This raises the intriguing possibility that the OpuCC substrate-binding protein (Fig. 1) will also productively interact with the core components of the OpuB system (and vice versa for OpuBC) in *B. subtilis* wild-type strains harboring simultaneously intact OpuB and OpuC transporters as high environmental osmolarity induces the synthesis of both of them (Kappes *et al*., 1999). It is however worth noting in this context that the *opuB* and *opuC* operons are subjected to different types of transcriptional and post-transcriptional control. The choline-responsive GbsR repressor negatively controls *opuB* transcription while it does not affect that of *opuC* (Nau-Wagner *et al*., 2012). Conversely, the GbsR-related repressor OpcR regulates the transcription of both the *opuC* and *opuB* operons (Lee *et al*., 2013). However, in contrast to GbsR (Nau-Wagner *et al*., 2012), the physiological stimulus or the effector molecule for this MarR-type regulator is unknown. Furthermore, under inducing conditions of the SigB-controlled general stress regulon of *B. subtilis* (Nannapaneni *et al*., 2012), an *opuB* anti-sense RNA is produced while no such regulatory RNA is known to exist for the *opuC* operon (Nicolas *et al*., 2012).

Genetic, biochemical and structural analysis revealed the presence of low-affinity ligand-binding sites in the TMDs of the *E. coli* maltose/maltodextrin system (Shuman, 1982; Covitz *et al*., 1994; Khare *et al*., 2009; Bordignon *et al*., 2010; Cui *et al*., 2010; Chen, 2013) and of the arginine/histidine ABC transporter from the thermophile *T. tengcongensis* (Yu *et al*., 2015), both of which belong to the type-I subfamily of ABC import systems (Locher, 2016; Lewinson and Livnat-Levanon, 2017). Mutational analysis of the internal binding sites in the MalF and MalG TMDs revealed that it is essential for the functioning of the maltose/maltodextrin ABC transporter (Covitz *et al*., 1994; Ehrle *et al*., 1996; Steinke *et al*., 2001; Khare *et al*., 2009). Telling in this regard is also the analysis of the high-affinity *myo*-inositol IbpA periplasmic binding protein from *C. crescentus* (Herrou and Crosson, 2013). This substrate-binding-protein could be converted through site-directed mutagenesis into a high-affinity ligand-binding protein for ribose, but the genetic combination of the *ibpA* ribose binding allele with the genes for the core components of the *myo*-inositol IatP-IatA ABC transporter did not allow enhanced growth of *C. crescentus* with ribose (Herrou and Crosson, 2013).

Assuming that low-affinity secondary substrate binding sites exist in the TMDs of the type-I ABC transporters OpuB and OpuC from *B. subtilis* as well, it is safe to state that they are insufficient to confer transport activity onto transporters gutted for their substrate-binding protein (Supporting Information Fig. S3). These findings are fully consistent with data from prior studies addressing this question for the maltose/maltodextrin ABC transporter from *E. coli* (Shuman, 1982; Boos and Shuman, 1998). However, it has been possible to obtain suppressor variants of this transport system carrying single amino acid substitutions in the MalG/MalF TMDs

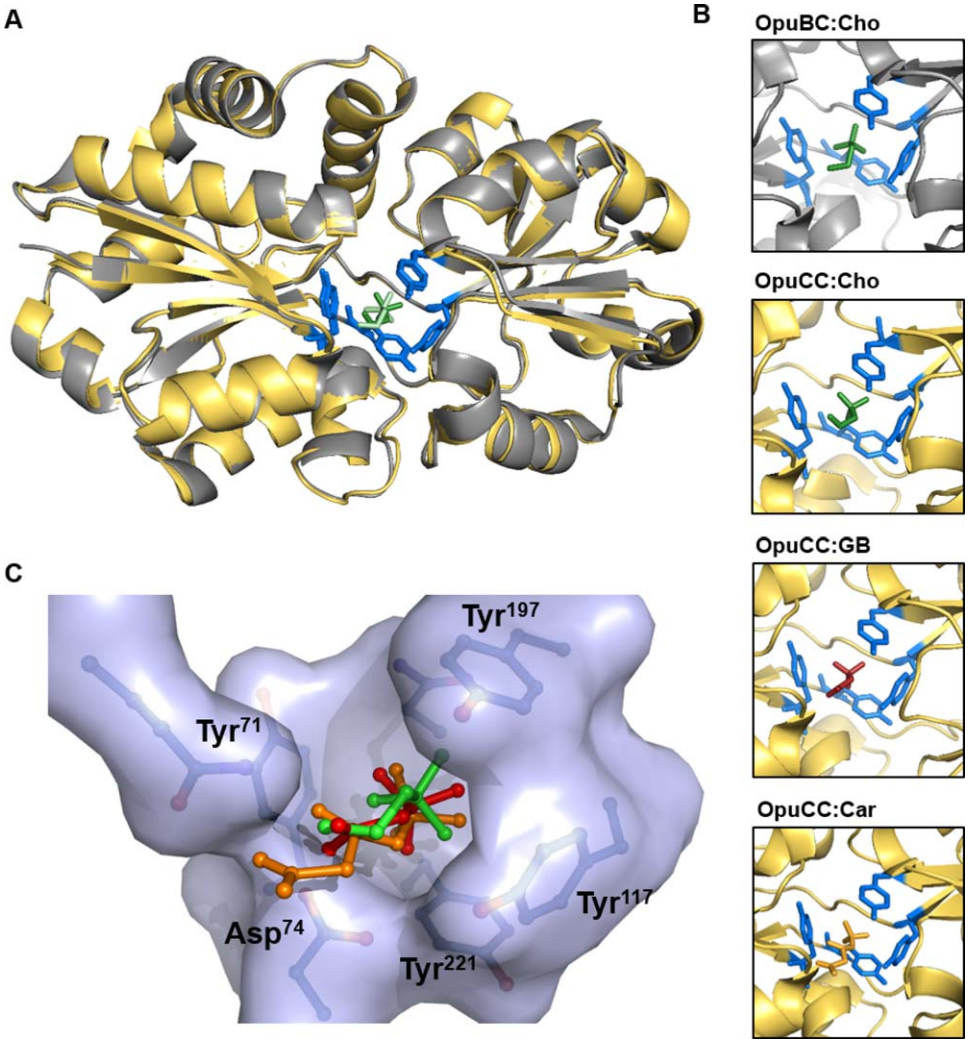

Fig. 6. Comparison of the OpuBC and OpuCC crystal structures and their ligand-binding sites.
A. Superimposition of the crystal structures of the OpuBC (gray) and OpuCC proteins (yellow) in complex with their common ligand choline (green sticks) (Du *et al.*, 2011; Pittelkow *et al.*, 2011). The side-chains of the four Tyr residues forming the "aromatic cage" (Bremer, 2011) are highlighted in blue; they are involved in coordinating the trimethlyammonium head-group of choline in OpuBC and OpuCC, and other ligands in OpuCC, within the binding sites via cation–π interactions (Du *et al.*, 2011; Pittelkow *et al.*, 2011; Mahadevi and Sastry, 2013). The residues forming the aromatic cage overlay perfectly in the OpuBC::choline and OpuCC::choline crystal structures.
B. Architecture of the ligand-binding pocket of OpuBC with choline (PDB accession number: 3R6U) and that of OpuCC in complex with choline (Cho) (PDB accession number: 3PPQ), glycine betaine (GB) (PDB accession number: 3PPP) and carnitine (Car) (PDB accession number: 3PPO) (Du *et al.*, 2011; Pittelkow *et al.*, 2011).
C. Superimposition of the OpuBC and OpuCC ligand-binding sites. The surface of the OpuBC protein is shown, and its aromatic cage (Tyr^{71}, Tyr^{117}, Tyr^{197}, Tyr^{221}) and the residue (Asp^{74}) critical for closing of the substrate-binding protein (Pittelkow *et al.*, 2011) are highlighted. The ligand choline (green) bound to OpuBC, and the ligands glycine betaine (red) and carnitine (orange) were extracted from OpuCC crystal structures (Du *et al.*, 2011) and are indicated as sticks. This visualization of the OpuBC binding pocket reveals a potential clash of the carboxy group of the OpuCC substrate glycine betaine with residue Asp^{74} when viewed in the context of the OpuBC ligand-binding site, while the OpuBC protein can accommodate carnitine.

allowing the Mal transporter to function without its cognate substrate-binding protein (MalE) (Covitz *et al.*, 1994). If an internal low-affinity substrate-binding site in the TMDs is required for the functioning of the promiscuous *B. subtilis* OpuC transporter, then it must also be present in the TMDs of the substrate-restricted OpuB system since the pairing of the core components of OpuB with the OpuCC binding protein confers substrate promiscuity (Figs 2 and 3). Hence, it might be of interest to search for the progenitor of the *B. subtilis* OpuB and OpuC ABC transporters among the *Bacilli* and study its substrate profile.

Crystallographic analysis of OpuBC and OpuCC (Fig. 6A) provided important clues with respect to the molecular determinants for the different substrate specificities of these two binding proteins (Du *et al.*, 2011; Pittelkow

et al., 2011). Their identical aromatic cage (Bremer, 2011) allows the binding of positively charged headgroups of various substrates through cation–π interactions (Du *et al*., 2011; Pittelkow *et al*., 2011; Mahadevi and Sastry, 2013; Bashir *et al*., 2014a,b; Broy *et al*., 2015) (Fig. 6B). This is visualized in Fig. 6C by overlaying the glycine betaine and carnitine ligands bound in the OpuCC crystal structure (Du *et al*., 2011) with that of choline trapped in the OpuBC crystal structure (Pittelkow *et al*., 2011). This overlay also reveals a clash of one of the oxygen atoms from the carboxylate of glycine betaine with the negatively charged side chain of Asp^{74} (predicted distance: 1.4 Å) (Fig. 6C). As this residue is critical for the closure of OpuBC upon entrapment of its choline ligand (Pittelkow *et al*., 2011), glycine betaine cannot be stably bound. In contrast, such a clash is not observed for carnitine (Fig. 6C), consistent with our finding that OpuB can import this osmostress protectant (Fig. 2). However, the carnitine derivatives γ-butyrobetaine and crotonobetaine are not substrates for the OpuB transporter but enter the cell exclusively via OpuC (Kappes and Bremer, 1998) (Figs 1–3). It is thus apparent, that further studies are required to fully understand the structural determinants for the substrate specificities of the OpuBC and OpuCC ligand-binding proteins.

In contrast to the functional characteristics of the hybrid OpuC::OpuBC system (Table 1), the OpuB::OpuCC transporter provided incomplete osmostress protection when benchmarked against a strain possessing the native OpuC transporter (Table 1; Fig. 3). We traced this limitation to a low cellular level of the xenogenetic OpuCC ligand-binding protein through Western blot analysis (Fig. 4A). Building on this finding and osmostress protection growth data (Figs 2, 3 and 4B), we developed a genetic suppressor screen that selected for faster growing colonies when only a very low amount (50 μM) of the osmostress protectant glycine betaine was provided (Fig. 4B–D). Through this screen, we found point mutations in the *gbsR* regulatory gene that lead to the synthesis of either partially (M2 and M3) or fully defective (M1) GbsR repressor proteins (Fig. 5). Hence, increased synthesis of the xenogenetic OpuCC ligand-binding protein in the suppressor strains can readily be understood in molecular terms since the transcription of the *opuB::opuCC* hybrid operon will be de-repressed in the mutant *gbsR* strains (Nau-Wagner *et al*., 2012) (Fig 5B). The de-repression of *opuB::opuCC* transcription in the *gbsR* suppressor strains will not only increase the amounts of the OpuCC binding protein but will simultaneously increase the amounts of the core components of the hybrid transporter, which might jointly lead to the better performance of the OpuB::OpuCC system under severe osmotic stress conditions (compare the growth of the parent LTB1 with that of the three suppressor strains LTB3, LTB4 and LTB5; Fig. 3).

When Ray *et al*. reported on the crystal structure of the *M. jannaschii* Mj233 protein, the template on which the *in silico* model of GbsR is based (Fig. 5A) (Nau-Wagner *et al*., 2012), the authors noted that the obtained structure is incompatible with binding of the Mj233 protein to a typical B-form of DNA (Ray *et al*., 2003). Modeling performed by Ray *et al*. suggests that very substantial topological re-arrangements of the homo-dimeric protein are required to allow DNA binding and that the long flexible linker region connecting the dimerization domain with the DNA-reading head in the Mj233 monomer will play a key role for these spatial re-orientations (Ray *et al*., 2003). We note with great interest, that the M2 and M3 suppressor mutations are located in the corresponding linker region in GbsR (Fig. 5A), a segment of this MarR-type repressor thought to transmit the inducer (choline)-mediated detachment from its operator sequence in *gbsAB* and *opuB* regulatory regions (Nau-Wagner *et al*., 2012). Serendipitously, our selection scheme for increased performance of the hybrid OpuB::OpuCC ABC transporter under osmotic stress conditions (Fig. 4C) has thus opened up a novel route to genetically study the structure/function relationship of the *B. subtilis* GbsR repressor through suppressor analysis.

Experimental procedures

Chemicals

The antibiotics ampicillin, chloramphenicol, erythromycin, kanamycin, spectinomycin, tetracycline and the chromogenic substrate para-nitrophenyl-α-glucopyranoside (pNPG) for the TreA enzyme assays were all obtained from Sigma-Aldrich (Steinheim, Germany). Radiolabeled [1-^{14}C]-glycine betaine (55 mCi mmol^{-1}) was purchased from American Radiolabeled Chemicals (St. Louis, MO). [*methyl*-^{14}C]-choline chloride (55 mCi mmol^{-1}) and [*N-methyl*-^{14}C]-carnitine hydrochloride (57 mCi mmol^{-1}) were obtained from Perkin-Elmer LAS GmbH (Rodgau, Germany). The sources of the compatible solutes used in this study have been described previously (Hoffmann and Bremer, 2011).

Media and growth conditions

E. coli and *B. subtilis* strains were routinely maintained on Luria Bertani (LB) agar plates, or cultured in LB liquid medium at 37°C (Miller, 1972). Chloramphenicol (10 μg ml^{-1}), erythromycin (1 μg ml^{-1}), kanamycin (5 μg ml^{-1}), spectinomycin (100 μg ml^{-1}) and tetracycline (10 μg ml^{-1}) were added to solid and liquid growth media used to propagate *B. subtilis* strains carrying chromosomal mutant alleles marked with an antibiotic resistance cassette. For

osmostress protection growth assays, transport assays and Western blot analysis, *B. subtilis* strains were cultivated in Spizizen's minimal medium (SMM) with 0.5% (wt/vol) glucose as carbon source and L-tryptophan (20 mg liter^{-1}) and L-phenylalanine (18 mg liter^{-1}) to satisfy the auxotrophic requirements of the domesticated wild-type strain JH642 (*trpC2 pheA1*) (Smith *et al.*, 2014) and its mutant derivatives (Supporting Information Table S1). A solution of trace elements was added to SMM to improve the growth of *B. subtilis* strains (Harwood and Archibald, 1990). The osmolarity of SMM was increased by the addition of NaCl from a 5 M stock solution. Solutions of compatible solutes were sterilized by filtration (Filtropur S 0.2 μm; Sarstedt, Nümbrecht, Germany) and were added to growth media from 100 mM stocks. All *B. subtilis* strains were inoculated from exponentially growing pre-cultures (propagated in SMM) to optical densities (OD_{578}) of about 0.1. The freshly inoculated cultures were grown at 37°C in a shaking water bath set to 220 rpm. All strains were grown in 20-ml culture volumes in 100-ml Erlenmeyer flasks.

Construction of hybrid opuB *and* opuC *gene clusters*

A high-fidelity DNA polymerase (Phusion High-Fidelity DNA Polymerase from New England Biolabs, Ipswich, MA) was used to amplify all DNA fragments, including both inserts and vectors, in a procedure similar to that described previously (Chen *et al.*, 2010). The DNA primers used for these experiments are listed in Supporting Information Table S2. Generally, primers used for amplifying inserts, or self-ligating PCR products, were first treated with T4 polynucleotide kinase (PNK, from Promega, Madison, Wi), which will add a phosphate to the 5′-ends of the PCR products and enable their subsequent ligations with dephosphorylated linear plasmid DNA, or another PCR product amplified with unmodified primers. To facilitate the expression and further genetic manipulation (e.g., deletion or swapping of the *opuBC* and *opuCC* genes) of the OpuB and OpuC ABC transporters, we first cloned the full length *opuB* or *opuC* operon (Kappes *et al.*, 1999), amplified by the primer pairs opuBF/opuBR, opuCF/opuCR, respectively (Supporting Information Table S2), into the vector pX (Kim *et al.*, 1996). Inserts present in this cloning vector can be stably integrated into the *B. subtilis* chromosome in a single copy into the non-essential *amyE* gene via double homologous recombination events between identical 5′- and 3′-segments of the *amyE* gene present on plasmid pX and the *B. subtilis* chromosome (Kim *et al.*, 1996). DNA of plasmid pX for the cloning experiments was generated by PCR amplification using a single forward primer pXF and either one of the two reverse primers (pXR or pXRb) (Supporting Information Table S2). PCR products amplified by pXF/pXRb are 566 bp longer than those by pXF/pXR. Neither one will amplify the 5′ end of *xylR* gene, thus removing this undesired DNA fragment from the final constructs. The residual intact pX plasmids were removed from the reaction mixture by digesting the PCR products with *DpnI* prior to further DNA purification (PCR purification kit, QIAGEN) and ligation (T4 DNA ligase, Roche). Colony PCR and subsequent DNA sequencing confirmed the successful construction of the desired plasmids. These cloning steps yielded plasmids pChen1 (*opuB*$^{+}$) and pChen3 (*opuC*$^{+}$) (Supporting Information Table S3).

To remove the coding regions for the *opuBC* and *opuCC* ligand-binding proteins from the corresponding *opu* operons, we designed outward-facing primers with priming sites immediately outside the targeted gene (*opuBC* or *opuCC* genes); such primers are likely suboptimal in their thermodynamic properties and may not be able to amplify circular plasmid. To facilitate amplification of the plasmids, we first digested the template plasmid, pChen1 and pChen3, with restriction enzyme *BglI* or *AgeI*, which produces a single cut inside *opuBC* or *opuCC* gene respectively. Polynucleotide-kinase-treated primer pairs, opuBClessF/opuBClessR (for the removal of *opuBC*) and opuCClessF/opuCClessR (for the removal of *opuCC*), were used to amplify the linearized pChen1 and pChen3 plasmids respectively. Subsequent *DpnI* digestion (to remove residual plasmid template), DNA purification and ligation produced plasmids pChen10 (*opuB* without *opuBC* gene) and pChen11 (*opuC* without *opuCC* gene). The deletion of the *opuBC* and *opuCC* genes from plasmids pChen1 and pChen3 (Supporting Information Table S3) and the absence of additional undesired mutations were ascertained by DNA sequence analysis.

To generate hybrid transporters, in which the ligand-binding protein OpuBC within the OpuB transporter is replaced by the OpuCC binding protein, or a vice versa construct, we used untreated primer pairs, opuBClessF/opuBClessR and opuCClessF/opuCClessR, to amplify linearized plasmids pChen1 and pChen3 (Supporting Information Table S3) respectively. The full length of *opuBC* and *opuCC* genes were amplified from genomic DNA of *B. subtilis* strain 168 using polynucleotide-kinase-treated primers opuBCF/opuBCR and opuCCF/opuCCR (Supporting Information Table S2) respectively. Subsequent cloning steps produced two plasmids, pChen5 (*opuB* with *opuCC* gene) and pChen6 (*opuC* with *opuBC* gene) with the replacements confirmed by DNA sequencing. However, plasmid pChen5 (Supporting Information Table S3) possesses an undesired point mutation in codon 211 (ATG to ATA) of the *opuCC* gene. Since this mutation leads to an amino acid substitution (Met^{211}/Ile) in the mature OpuCC protein (Supporting Information Fig. S7), it was corrected back to the wild-type sequence via site-directed mutagenesis (using the Q5 Site-Directed Mutagenesis Kit, New Englang BioLabs, Ipswich, MA) and a set of custom-synthesized mutagenesis primers (primer Q5_OpuCCMut_TzuC_F and primer Q5_OpuCCMut_TzuC_R) (Supporting Information Table S2). The resulting plasmid was pLT1 (Supporting Information Table S3); the correctness of the genomic DNA inserted into this plasmid was verified by DNA sequence analysis.

Construction of the TMB118 chassis strain

Mutants carrying chromosomal full-length deletions of the *opuA*-, *opuB*- and *opuC*-operons were constructed using long-flanking region PCR (Kuwayama *et al.*, 2002). The primers for the amplification of the 5′- and the 3′-regions flanking the gene of interest or of the antibiotic resistance cassettes are listed in Supporting Information Table S2.

The tetracycline resistance cassette inserted into the *opuA* locus, the erythromycin resistance cassette inserted into the *opuB* locus, and the spectinomycin resistance cassette inserted into the *opuC* locus were amplified using the plasmids pDG1515, pDG646 and pDG1726 (Guerout-Fleury *et al*., 1995) as the templates, respectively. For each *opu*-deletion construct, fusion PCR products consisting of the 5′-flanking region, the antibiotic resistance cassettes, and the 3′-flanking region were used to transform *B. subtilis* wild-type JH642 and plated on LB agar plates containing the appropriate antibiotic. After purification of individual transformants on LB agar plates containing the appropriate antibiotic, chromosomal DNA was prepared from these strains and used to verify the correct insertion of the desired *opu* deletions into the chromosome of the *B. subtilis* strain JH642 by PCR using primers flanking the deletion/insertion mutation. The resulting mutant strains were TMB107 [Δ(*opuA*::*tet*)3], TMB116 [Δ(*opuB*::*ery*)1] and TMB108 [Δ(*opuC*::*spc*)3] (Supporting Information Table S1). For the construction of a quadruple knock-out strain carrying deletions in all glycine betaine and choline uptake systems of *B. subtilis* (Hoffmann and Bremer, 2017), we used the JH642-derived *opuD* deletion strain RMKB7 [(Δ*opuD*::*kan*)2] (Kappes *et al*., 1996) as the starting recipient for sequential transformations with chromosomal DNA of the individual *opu* deletion mutants and by selecting for the appropriate antibiotic resistance marker (Supporting Information Table S1). The resulting quadruple *opu* deletion mutant strain was TMB118 [*opuA opuB opuC opuD*] (Supporting Information Table S1). From the five Opu transporters operating in *B. subtilis* (Hoffmann and Bremer, 2017), only the osmostress responsive proline-specific OpuE system (von Blohn *et al*., 1997) is intact in strain TMB118, thereby preventing loss of the newly synthesized osmostress protectant L-proline from continuously high-salinity challenged strains (Brill *et al*., 2011; Hoffmann *et al*., 2012).

Isolation and characterization of suppressor mutants improving the efficiency of the hybrid OpuB::OpuCC transporter

To isolate mutants that show enhanced transport capacity for glycine betaine via the hybrid OpuB::OpuCC transport system, cells of *B. subtilis* strain LTB1 (Supporting Information Table S1) were grown in SMM supplemented with 0.4 M NaCl. After reaching exponential growth phase (OD_{578} of 2), cells were plated in serial dilutions onto high-salt agar plates (SMM containing 1.1 M NaCl) and a low concentration (50 μM) of the osmostress protectant glycine betaine. Strain LTB1 cannot grow under these conditions but suppressor mutant strains grew after about five days of incubation at 37°C. The frequency by which these suppressor strains appear was estimated by plating cells of strains CCB3 ($OpuC^+$) and LTB1 (OpuB::OpuCC*) from four independently grown cultures in SMM containing 0.4 M NaCl onto SMM agar plates containing 1.1 M NaCl and 50 μM glycine betaine and by comparing the plating efficiency of these strains on this medium with that on SMM agar plates containing 0.4 M NaCl and 50 μM glycine betaine. Both the CCB3 ($OpuC^+$) and LTB1 (OpuB::OpuCC*) strains plated with the same efficiency on SMM agar plates containing 0.4 M NaCl and 50 μM glycine betaine since the degree of the imposed osmotic stress is very mild for *B. subtilis* (Boch *et al*., 1994).

Colonies of three independently isolated suppressor strains LTB3 (M1), LTB4 (M2) and LTB5 (M3) (Supporting Information Table S1) were purified by streaking them on the same medium used for their isolation. Chromosomal DNA was prepared from them using routine procedures (Cutting and Vander Horn, 1990). The isolated chromosomal DNA was then used to amplify the complete *opuB::opuCC* hybrid operon and the *gbsR* gene by PCR using primer combinations listed in Supporting Information Table S2. DNA-sequence analysis of these PCR products was carried out by MWG Eurofins GmbH (Ebersberg, Germany). While the *opuB::opuCC* hybrid operon present in the LTB3, LTB4 and LTB5 suppressor strains perfectly matched that present in their parent strain LTB1, each of them carried point mutations in *gbsR* resulting in single amino acid substitutions in the GbsR repressor protein. Strains LTB3, LTB4 and LTB5 carried the following *gbsR* alleles: GGG/GAG [Gly^{39}/Glu; M1], ACA/GCA [Thr^{79}/Ala; M2] and CGC/AGC [Arg^{85}/Ser; M3].

Constructions of treA *reporter gene fusion strains*

A 1167-bp DNA fragment containing the entire *gbsR* gene and the first part of the *gbsA* gene was cut with *Ssp*I out of plasmid pJB007 (Boch *et al*., 1996; Nau-Wagner *et al*., 2012) and was cloned into the *Sma*I opened *bgaB*-reporter fusion plasmid pFSB1 in which the *gbsA-bgaB* reporter fusion is flanked by the 5-′ and 3′-segements of the *B. subtilis amyE* gene (Supporting Information Table S3). In the resulting plasmid pGNB2, the *bgaB* reporter gene was then replaced with a *treA* reporter gene (Schöck *et al*., 1996) through a deletion of a *Bam*HI-*Sac*I DNA fragment and subsequent insertion of the *treA* gene that was retrieved from plasmid pJMB1 (Supporting Information Table S3) using the same combination of restriction enzymes. The resulting plasmid was pGNB13, which carries an intact *gbsR* gene and a *gbsA-treA* reporter fusion (Supporting Information Table S3). The three M1, M2 and M3 mutations were then inserted into the *gbsR* gene present on plasmid pGNB13 using the Q5 Site-Directed Mutagenesis Kit (New England BioLabs, Ipswich, MA) and a series of custom-synthesized mutagenesis primers (purchased from Microsynth, Lindau, Germany). The presence of the desired mutations in the *gbsR* gene was confirmed by DNA sequencing. Plasmids pLT2, pLT3 and pLT4 carry the following alterations in *gbsR*: GGG/GAG [Gly^{39}/Glu; M1], ACA/GCA [Thr^{79}/Ala; M2] and CGC/AGC [Arg^{85}/Ser; M3] respectively. The *gbsR gbsA′-treA* reporter constructs present in these plasmids are followed by a chloramphenicol resistance gene and the entire construct is flanked by the 5′- and 3′-segments of the *amyE* gene. This allows the integration of the various *gbsR gbsA′-treA* constructs as a single copy into the chromosomal *amyE* locus of the *B. subtilis* strain GNB40 (*gbsR::neo*^{R}) (Supporting Information Table S1) (Nau-Wagner *et al*., 2012) via transformation with linearized plasmid DNA and selection for chloramphenicol-resistant transformants. This yielded strains GNB51 ($gbsR^+$), LTB11 (*gbsR-*

Gly^{39}/Glu; M1), LTB12 (*gbsR*-Thr^{79}/Ala; M2) and LTB17 (*gbsR*-Arg^{85}/Ser; M3) (Supporting Information Table S1).

The wild-type *gbsR* gene was cloned into plasmid pBB287 (a kind gift from Dr. David Rudner, Harvard Medical School; USA) using a DNA fragment amplified from chromosomal DNA of strain JH642 using the gbsR-F and gbsR-R combination of DNA primers (Supporting Information Table S2) thereby yielding plasmid pTL5. We then introduced the above described three *gbsR* mutant alleles into the resulting *gbsR*$^+$ plasmid pLT5 (Supporting Information Table S3) via site-directed mutagenesis [resulting in plasmids pLT6 (*gbsR*-Gly^{39}/Glu; M1), pLT7 (*gbsR*-Thr^{79}/Ala; M2) and pLT8 (*gbsR*-Arg^{85}/Ser; M3)] (Supporting Information Table S3), and verified the presence of the desired mutations and the absence of secondary alterations by DNA sequence analysis. In plasmids pLT5, pLT6, pLT7 and pLT8, the *gbsR* genes are flanked by the 5′ and 3′ segments of the *ytoI* gene of *B. subtilis*, which allows their stable integration as a single copy into the non-essential *ytoI* locus via a double homologous recombination event. The *B. subtilis* strain into which the wild-type *gbsR* gene and its mutant alleles were introduced into the *ytoI* locus via transformation was STHB53, a strain carrying a genetically stable, single-copy *opuB-treA* reporter gene fusion at the *amyE* locus and that was simultaneously defective in the *gbsR* gene (Supporting Information Table S1). As a result, the influence of the wild-type and mutant *gbsR* genes present at the *ytoI* locus on *opuB* expression (Nau-Wagner *et al*., 2012) can be assessed though *opuB-treA* reporter gene assays in an isogenic set of strains. The *B. subtilis* strains resulting from these genetic manipulations were LTB18 (*gbsR*$^+$), LTB19 (*gbsR*-Gly^{39}/Glu; M1), LTB20 (*gbsR*-Thr^{79}/Ala; M2) and LTB21 (*gbsR*-Arg^{85}/Ser; M3) (Supporting Information Table S1).

Reporter-fusion analysis

The reporter fusions used in this study rely on the salt-tolerant TreA [phospho-α-(1,1)-glucosidase] enzyme whose activity can be quantitated using the chromogenic substrate pNPG (Gotsche and Dahl, 1995; Schöck *et al*., 1996). In these operon fusions, expression of the promoter-less *treA* reporter gene is dependent on the transcriptional activity of the promoter of interest; the fused *treA* carries its authentic ribosome-binding site. All *treA* reporter fusions used in this study are present in a single copy stably integrated into the genome of *B. subtilis* strains carrying a chromosomal *treA* gene disruption mutation (Supporting Information Table S1). Aliquots (1.5 ml) from *B. subtilis treA* fusion reporter strains were withdrawn from cultures and their TreA enzyme activity was measured with the aid of the chromogenic substrate pNPG as described previously (Gotsche and Dahl, 1995; Nau-Wagner *et al*., 2012). TreA specific enzyme activity is expressed in units per mg of protein. Protein concentrations were estimated from the optical density of the cell culture (Miller, 1972).

Immunoblot analysis

Total cell extracts from various *B. subtilis* cultures were prepared as described previously (Kempf and Bremer, 1995). Each cell suspension was adjusted to an OD_{578} of 10 with a 10 mM Tris – 1 mM EDTA (TE) buffer solution containing 10 mg ml^{-1} lysozyme. After 5 min of incubation of this mixture at 37°C, lysed cells were treated with twofold concentrated SDS sample buffer [62.5 mM Tris-HCl (pH 6.8), 2.5% SDS, 0.002% bromphenol blue, 0.71 M β-mercapto-ethanol]. Equal volumes of protein samples prepared from the lysed *B. subtilis* cells were separated by electrophoresis on a 13.5% SDS-polyacrylamide gel (13.5 cm × 26.5 cm). Proteins were then transferred to a methanol-activated PVDF membrane (EMD Millipore, Bedford, MA) by semidry blotting. Membranes were blocked in TBSTM [20 mM Tris (pH 7.5), 5% milk, 150 mM NaCl, 0.05% Tween-20] over night and the bound proteins were then probed with a rabbit polyclonal OpuBC (diluted 1:2000 in TBSTM) or OpuCC (diluted 1:1250 in TBSTM) antiserum for 1 h (Kappes *et al*., 1999). The formed protein-antibody complexes were subsequently detected with a goat anti-rabbit immunoglobulin G-alkaline phosphatase-conjugated secondary antibody (Promega, Madison, WI), using CDP-Star (Roche Diagnostics GmbH, Mannheim, Germany) as a chemiluminescent substrate. It should be noted that the used polyclonal OpuBC and OpuCC anti-sera recognize their substrates with different specificities. The OpuBC anti-serum recognizes effectively OpuBC, weakly the amino acid sequence-related OpuCC protein and cross-reacts with an unknown *B. subtilis* protein, a contaminating activity which was already present in the pre-serum (Kappes *et al*., 1999). The OpuCC anti-serum does not recognize the OpuBC protein (Kappes *et al*., 1999) (Supporting Information Fig. S4).

Transport assays with radiolabeled substrates

To determine kinetic parameters of different Opu transporters, the uptake of [1-^{14}C]glycine betaine, [*methyl*-^{14}C]choline chloride and [*N-methyl*-^{14}C]carnitine hydrochloride was measured. Cultures of various *B. subtilis* strains were grown in SMM at 37°C containing 0.4 M NaCl to an OD_{578} of 0.3 and used immediately for the transport assay. The substrate concentration was varied between 3 μM and 120 μM for glycine betaine, between 3 μM and 500 μM for choline, and between 3 μM and 13 mM for carnitine. The unlabeled compounds were spiked with 1 μM of the radiolabeled substrate used in the particular transport assays. Uptake assays were conducted at 37°C. The import of the radiolabeled substrate was followed over time, and the amount of radiolabeled substrate that was taken up by the *B. subtilis* cells was determined by scintillation counting as described previously (Kempf and Bremer, 1995; Kappes *et al*., 1996).

Assessing the potential docking interfaces of the OpuBC and OpuCC binding proteins with their cognate TMDs

From the crystal structure analysis (PDB number 2ONK) of the type-I molybdate transporter (ModBC) from the archaeon *A. fulgidus* in complex with its substrate binding protein (ModA), the docking interface between ModA and the homo-dimeric ModB TMD component is known. In the structure of the entire ABC-transporter complex, ModA docks with each lobe onto one ModB monomer (Hollenstein

et al., 2007). Building on these data, we assessed the similarities and potential differences between the docking interfaces of the OpuBC and OpuCC proteins using the high-resolution crystal structures (OpuBC – 1.6 Å; OpuCC – 1.9 Å) of the OpuBC::choline (PDB code 3R6U) and OpuCC::choline (PDB code 3PPQ) complexes (Du *et al*., 2011; Pittelkow *et al*., 2011). An overlay of these two crystal structures (Fig. 6A) revealed a root-mean-square deviation (r.m.s.d) of only 0.6 Å over 256 C-alpha atoms. We then focused our analysis on the structural elements of OpuBC and OpuCC that will face the periplasmic membrane, as these regions of the binding proteins will be involved in interaction with the OpuBB/OpuBD and OpuCB/OpuCD TMDs components. We identified three regions in the two substrate-binding proteins that might interact with surface exposed regions of the TMDs. In OpuBC (Pittelkow *et al*., 2011) these are located in β-sheet 2 consisting of the sequence ^{41}LKTTTTIKNLG^{50} and the loop connecting helix 8–9 consisting of the amino acids ^{263}GNLKEP^{268} in lobe 1 and β-sheet 8 with the sequence ^{173}GTYPMQ^{178} in lobe 2 (Supporting Information Fig. S8B). Conducting such an analysis with the OpuCC protein (Du *et al*., 2011), we found a similar set of structural elements facing towards the OpuCB/OpuCD transmembrane components. Here, the amino acid sequences involved in interactions with the TMDs are ^{61}LNTALVKNL^{69} in β-sheet 2 and ^{283}GKLKEP^{288} in the loop connecting helix 8–9 in lobe 1. In lobe 2 the β-sheet is formed by the amino acid sequence ^{192}GTTYPMQ^{198} (Supporting Information Fig. S8B). An inspection of the charge on the surface of the two OpuBC and OpuCC lobes revealed that the docking interfaces of the two binding proteins are in all likelihood very similar, a finding that is fully consistent with the high degree of amino acid sequence identity between the OpuBB/OpuCB (85%) and OpuBD/OpuCD (85%) pairs of the TMDs from the OpuB and OpuC transporters respectively (Kappes *et al*., 1999)

Figure preparation of crystal structures

Figures of the crystal structures of the OpuBC and OpuCC ligand-binding proteins (Du *et al*., 2011; Pittelkow *et al*., 2011) were prepared with the PyMol software suite (www.pymol.org) (Delano, 2002) using crystallographic data summarized in the PDB files 3PPO (OpuCC::carnitine complex), 3PPP (OpuCC::glycine betaine complex), 3PPQ (OpuCC::choline complex) and 3RGU (OpuBC::choline complex).

Acknowledgements

Financial support for this study was provided by the LOEWE program of the state of Hessen (via the Center for Synthetic Microbiology, University of Marburg; to E.B.), a contribution of the Fonds der Chemischen Industrie (to E.B) and by the Strategischer Forschungsfond (SFF) (Heinrich-Heine-University Düsseldorf; to S.H.J.S.). We greatly appreciate the expert help of Vickie Koogle in the language editing of our manuscript. We thank David Rudner, Frank Spiegelhalter, Stefanie Ronzheimer, Gabriele Nau-Wagner and Sebastian Broy for kindly providing plasmids and bacterial strains.

Author contributions

E.B. conceived and directed this study. L.T. conducted most of the experiments. C.C. constructed plasmids of the original hybrid *opu* operons and performed exploratory experiments. T.H. constructed the *B. subtilis* TMB118 chassis strain and provided help with the transport assays and their analysis. S.H.J.S. and L.S. offered intellectual input into the interpretation of the data, and S.H.J.S. conducted modeling studies. E.B. and L.T. wrote the manuscript with input of all authors. All authors read and approved the manuscript.

Conflict of Interest

All authors declare that they have no conflict of interest.

References

Albers, S.V., Koning, S.M., Konings, W.N., and Driessen, A.J. (2004) Insights into ABC transport in archaea. *J Bioenerg Biomembr* **36**: 5–15.

Alvarez, F.J., Orelle, C., Huang, Y., Bajaj, R., Everly, R.M., Klug, C.S., and Davidson, A.L. (2015) Full engagement of liganded maltose-binding protein stabilizes a semi-open ATP-binding cassette dimer in the maltose transporter. *Mol Microbiol* **98**: 878–894.

Bashir, A., Hoffmann, T., Kempf, B., Xie, X., Smits, S.H., and Bremer, E. (2014a) The plant-derived compatible solutes proline betaine and betonicine confer enhanced osmotic and temperature stress tolerance to *Bacillus subtilis*. *Microbiology* **160**: 2283–2294.

Bashir, A., Hoffmann, T., Smits, S.H., and Bremer, E. (2014b) Dimethlyglycine provides salt and temperature stress protection to *Bacillus subtilis*. *Appl Environ Microbiol* **80**: 2773–2785.

Beis, K. (2015) Structural basis for the mechanism of ABC transporters. *Biochem Soc Trans* **43**: 889–893.

Berntsson, R.P., Smits, S.H., Schmitt, L., Slotboom, D.J., and Poolman, B. (2010) A structural classification of substrate-binding proteins. *FEBS Lett* **584**: 2606–2617.

Boch, J., Kempf, B., and Bremer, E. (1994) Osmoregulation in *Bacillus subtilis*: synthesis of the osmoprotectant glycine betaine from exogenously provided choline. *J Bacteriol* **176**: 5364–5371.

Boch, J., Kempf, B., Schmid, R., and Bremer, E. (1996) Synthesis of the osmoprotectant glycine betaine in *Bacillus subtilis*: characterization of the *gbsAB* genes. *J Bacteriol* **178**: 5121–5129.

Boos, W., and Shuman, H. (1998) Maltose/maltodextrin system of *Escherichia coli*: transport, metabolism, and regulation. *Microbiol Mol Biol Rev* **62**: 204–229.

Bordignon, E., Grote, M., and Schneider, E. (2010) The maltose ATP-binding cassette transporter in the 21st century – towards a structural dynamic perspective on its mode of action. *Mol Microbiol* **77**: 1354–1366.

Bourot, S., Sire, O., Trautwetter, A., Touze, T., Wu, L.F., Blanco, C., and Bernard, T. (2000) Glycine betaine-assisted protein folding in a *lysA* mutant of *Escherichia coli*. *J Biol Chem* **275**: 1050–1056.

Bouskill, N.J., Wood, T.E., Baran, R., Ye, Z., Bowen, B.P., Lim, H., *et al*. (2016) Belowground response to drought in a tropical forest soil. I. changes in microbial functional potential and metabolism. *Front Microbiol* **7**: 525.

Bremer, E. (2002) Adaptation to changing osmolarity. In *Bacillus Subtilis and Its Closes Relatives: From Genes to Cells*. Sonenshein, A.L., Hoch, J.A., and Losick, R. (eds). Washington, DC: ASM Press, pp. 385–391.

Bremer, E. (2011) Crystal ball – 2011. A look into the aromatic cage. *Environ Microbiol Rep* **3**: 1–5.

Bremer, E., and Krämer, R. (2000) Coping with osmotic challenges: osmoregulation through accumulation and release of compatible solutes. In *Bacterial Stress Responses*. Storz, G., and Hengge-Aronis, R. (eds). Washington, DC: ASM Press, pp. 79–97.

Brill, J., Hoffmann, T., Bleisteiner, M., and Bremer, E. (2011) Osmotically controlled synthesis of the compatible solute proline is critical for cellular defense of *Bacillus subtilis* against high osmolarity. *J Bacteriol* **193**: 5335–5346.

Broy, S., Chen, C., Hoffmann, T., Brock, N.L., Nau-Wagner, G., Jebbar, M., *et al*. (2015) Abiotic stress protection by ecologically abundant dimethylsulfoniopropionate and its natural and synthetic derivatives: insights from *Bacillus subtilis*. *Environ Microbiol* **7**: 2362–2378.

Chen, J. (2013) Molecular mechanism of the *Escherichia coli* maltose transporter. *Curr Opin Struct Biol* **23**: 492–498.

Chen, C., Malek, A.A., Wargo, M.J., Hogan, D.A., and Beattie, G.A. (2010) The ATP-binding cassette transporter Cbc (choline/betaine/carnitine) recruits multiple substrate-binding proteins with strong specificity for distinct quaternary ammonium compounds. *Mol Microbiol* **75**: 29–45.

Covitz, K.M., Panagiotidis, C.H., Hor, L.I., Reyes, M., Treptow, N.A., and Shuman, H.A. (1994) Mutations that alter the transmembrane signalling pathway in an ATP binding cassette (ABC) transporter. *EMBO J* **13**: 1752–1759.

Cui, J., Qasim, S., and Davidson, A.L. (2010) Uncoupling substrate transport from ATP hydrolysis in the *Escherichia coli* maltose transporter. *J Biol Chem* **285**: 39986–399893.

Cutting, S.M., and Vander Horn, P.B. (1990) Genetic analysis. In *Molecular Biological Methods for Bacillus*. Harwood, C.R., and Cutting, S.M. (eds). Chichester: John Wiley & Sons, pp. 27–74.

Daus, M.L., Berendt, S., Wuttge, S., and Schneider, E. (2007) Maltose binding protein (MalE) interacts with periplasmic loops P2 and P1 respectively of the MalFG subunits of the maltose ATP binding cassette transporter (MalFGK(2)) from *Escherichia coli* and *Salmonella* during the transport cycle. *Mol Microbiol* **66**: 1107–1122.

Davidson, A.L., Dassa, E., Orelle, C., and Chen, J. (2008) Structure, function, and evolution of bacterial ATP-binding cassette systems. *Microbiol Mol Biol Rev* **72**: 317–364.

Davidson, A.L., Shuman, H.A., and Nikaido, H. (1992) Mechanism of maltose transport in *Escherichia coli*: transmembrane signaling by periplasmic binding proteins. *Proc Natl Acad Sci U S A* **89**: 2360–2364.

Delano, W.L. (2002) *The PyMol Molecular Graphics System*. San Carlos, CA: Delano Scientific.

Du, Y., Shi, W.W., He, Y.X., Yang, Y.H., Zhou, C.Z., and Chen, Y. (2011) Structures of the substrate-binding protein provide insights into the multiple compatible solute binding specificities of the *Bacillus subtilis* ABC transporter OpuC. *Biochem J* **436**: 283–289.

Ehrle, R., Pick, C., Ulrich, R., Hofmann, E., and Ehrmann, M. (1996) Characterization of transmembrane domains 6, 7, and 8 of MalF by mutational analysis. *J Bacteriol* **178**: 2255–2262.

Eitinger, T., Rodionov, D.A., Grote, M., and Schneider, E. (2011) Canonical and ECF-type ATP-binding cassette importers in prokaryotes: diversity in modular organization and cellular functions. *FEMS Microbiol Rev* **35**: 3–67.

Ghimire-Rijal, S., Lu, X., Myles, D.A., and Cuneo, M.J. (2014) Duplication of genes in an ATP-binding cassette transport system increases dynamic range while maintaining ligand specificity. *J Biol Chem* **289**: 30090–30100.

Gotsche, S., and Dahl, M.K. (1995) Purification and characterization of the phospho-alpha-(1,1)-glucosidase (TreA) of *Bacillus subtilis* 168. *J Bacteriol* **177**: 2721–2726.

Gouridis, G., Schuurman-Wolters, G.K., Ploetz, E., Husada, F., Vietrov, R., de Boer, M., *et al*. (2015) Conformational dynamics in substrate-binding domains influences transport in the ABC importer GlnPQ. *Nat Struct Mol Biol* **22**: 57–64.

Grote, M., Polyhach, Y., Jeschke, G., Steinhoff, H.J., Schneider, E., and Bordignon, E. (2009) Transmembrane signaling in the maltose ABC transporter MalFGK2-E: periplasmic MalF-P2 loop communicates substrate availability to the ATP-bound MalK dimer. *J Biol Chem* **284**: 17521–17526.

Guerout-Fleury, A.M., Shazand, K., Frandsen, N., and Stragier, P. (1995) Antibiotic-resistance cassettes for *Bacillus subtilis*. *Gene* **167**: 335–336.

Harwood, C.R., and Archibald, A.R. (1990) Growth, maintenance and general techniques. In *Molecular Biological Methods for Bacillus*. Harwood, C.R., and Cutting, S.M. (eds). Chichester: John Wiley & Sons, pp. 1–26.

Hekstra, D., and Tommassen, J. (1993) Functional exchangeability of the ABC proteins of the periplasmic binding protein-dependent transport-systems Ugp and Mal of *Escherichia coli*. *J Bacteriol* **175**: 6546–6552.

Herrou, J., and Crosson, S. (2013) myo-inositol and d-ribose ligand discrimination in an ABC periplasmic binding protein. *J Bacteriol* **195**: 2379–2388.

Higgins, C.F. (1992) ABC transporters: from microorganisms to man. *Annu Rev Cell Biol* **8**: 67–113.

Higgins, C.F., and Ames, G.F. (1981) Two periplasmic transport proteins which interact with a common membrane receptor show extensive homology: complete nucleotide sequences. *Proc Natl Acad Sci U S A* **78**: 6038–6042.

Hoffmann, T., and Bremer, E. (2011) Protection of *Bacillus subtilis* against cold stress via compatible-solute acquisition. *J Bacteriol* **193**: 1552–1562.

Hoffmann, T., and Bremer, E. (2016) Management of osmotic stress by *Bacillus subtilis*: genetics and physiology. In *Stress and Environmental Regulation of Gene Expression and Adaptation in Bacteria*. de Bruijn, F.J. (ed). Wiley-Blackwell Publishers, pp. 657–676.

Hoffmann, T., and Bremer, E. (2017) Guardiens in a stressful world: the Opu family of compatible solute transporters from *Bacillus subtilis*. *Biol Chem* **398**: 193–214.

Hoffmann, T., von Blohn, C., Stanek, A., Moses, S., Barzantny, S., and Bremer, E. (2012) Synthesis, release, and recapture of the compatible solute proline by osmotically stressed *Bacillus subtilis* cells. *Appl Environ Microbiol* **78**: 5753–5762.

Hollenstein, K., Frei, D.C., and Locher, K.P. (2007) Structure of an ABC transporter in complex with its binding protein. *Nature* **446**: 213–216.

Holtmann, G., and Bremer, E. (2004) Thermoprotection of *Bacillus subtilis* by exogenously provided glycine betaine and structurally related compatible solutes: involvement of Opu transporters. *J Bacteriol* **186**: 1683–1693.

Hopfner, K.P. (2016) Architectures and mechanisms of ATP binding cassette proteins. *Biopolymers* **105**: 492–504.

Horn, C., Sohn-Bösser, L., Breed, J., Welte, W., Schmitt, L., and Bremer, E. (2006) Molecular determinants for substrate specificity of the ligand-binding protein OpuAC from *Bacillus subtilis* for the compatible solutes glycine betaine and proline betaine. *J Mol Biol* **357**: 592–606.

Ignatova, Z., and Gierasch, L.M. (2006) Inhibition of protein aggregation *in vitro* and *in vivo* by a natural osmoprotectant. *Proc Natl Acad Sci U S A* **103**: 13357–13361.

Kappes, R.M., and Bremer, E. (1998) Response of *Bacillus subtilis* to high osmolarity: uptake of carnitine, crotonobetaine and butyrobetaine via the ABC transport system OpuC. *Microbiology* **144**: 83–90.

Kappes, R.M., Kempf, B., and Bremer, E. (1996) Three transport systems for the osmoprotectant glycine betaine operate in *Bacillus subtilis*: characterization of OpuD. *J Bacteriol* **178**: 5071–5079.

Kappes, R.M., Kempf, B., Kneip, S., Boch, J., Gade, J., Meier-Wagner, J., and Bremer, E. (1999) Two evolutionarily closely related ABC transporters mediate the uptake of choline for synthesis of the osmoprotectant glycine betaine in *Bacillus subtilis*. *Mol Microbiol* **32**: 203–216.

Kempf, B., and Bremer, E. (1995) OpuA, an osmotically regulated binding protein-dependent transport system for the osmoprotectant glycine betaine in *Bacillus subtilis*. *J Biol Chem* **270**: 16701–16713.

Kempf, B., and Bremer, E. (1998) Uptake and synthesis of compatible solutes as microbial stress responses to high osmolality environments. *Arch Microbiol* **170**: 319–330.

Kempf, B., Gade, J., and Bremer, E. (1997) Lipoprotein from the osmoregulated ABC transport system OpuA of *Bacillus subtilis*: purification of the glycine betaine binding protein and characterization of a functional lipidless mutant. *J Bacteriol* **179**: 6213–6220.

Khare, D., Oldham, M.L., Orelle, C., Davidson, A.L., and Chen, J. (2009) Alternating access in maltose transporter mediated by rigid-body rotations. *Mol Cell* **33**: 528–536.

Kim, L., Mogk, A., and Schumann, W. (1996) A xylose-inducible *Bacillus subtilis* integration vector and its application. *Gene* **181**: 71–76.

Korkhov, V.M., Mireku, S.A., Hvorup, R.N., and Locher, K.P. (2012a) Asymmetric states of vitamin B(12) transporter BtuCD are not discriminated by its cognate substrate binding protein BtuF. *FEBS Lett* **586**: 972–976.

Korkhov, V.M., Mireku, S.A., and Locher, K.P. (2012b) Structure of AMP-PNP-bound vitamin B12 transporter BtuCD-F. *Nature* **490**: 367–372.

Kuan, G., Dassa, E., Saurin, W., Hofnung, M., and Saier, M.H. Jr. (1995) Phylogenetic analyses of the ATP-binding constituents of bacterial extracytoplasmic receptor-dependent ABC-type nutrient uptake permeases. *Res Microbiol* **146**: 271–278.

Kuwayama, H., Obara, S., Morio, T., Katoh, M., Urushihara, H., and Tanaka, Y. (2002) PCR-mediated generation of a gene disruption construct without the use of DNA ligase and plasmid vectors. *Nucleic Acids Res* **30**: E2.

Lee, C.H., Wu, T.Y., and Shaw, G.C. (2013) Involvement of OpcR, a GbsR-type transcriptional regulator, in negative regulation of two evolutionarily closely related choline uptake genes in *Bacillus subtilis*. *Microbiology* **159**: 2087–2096.

Leonard, B.A., Podbielski, A., Hedberg, P.J., and Dunny, G.M. (1996) *Enterococcus faecalis* pheromone binding protein, PrgZ, recruits a chromosomal oligopeptide permease system to import sex pheromone cCF10 for induction of conjugation. *Proc Natl Acad Sci U S A* **93**: 260–264.

Lewinson, O., and Livnat-Levanon, N. (2017) Mechanism of action of ABC importers: conservation, divergence, and physiological adaptations. *J Mol Biol* **429**: 606–619.

Locher, K.P. (2016) Mechanistic diversity in ATP-binding cassette (ABC) transporters. *Nat Struct Mol Biol* **23**: 487–493.

Mahadevi, A.S., and Sastry, G.N. (2013) Cation–pi interaction: its role and relevance in chemistry, biology, and material science. *Chem Rev* **113**: 2100–2138.

Mao, B., Pear, M.R., McCammon, J.A., and Quiocho, F.A. (1982) Hinge-bending in l-arabinose-binding protein. The "Venus's-flytrap" model. *J Biol Chem* **257**: 1131–1133.

Miller, J.H. (1972) *Experiments in Molecular Genetics*. Cold Spring Harbor, NY: Cold Spring Harbor Laboratory.

Nannapaneni, P., Hertwig, F., Depke, M., Hecker, M., Mäder, U., Völker, U., *et al*. (2012) Defining the structure of the general stress regulon of *Bacillus subtilis* using targeted microarray analysis and random forest classification. *Microbiology* **158**: 696–707.

Nau-Wagner, G., Opper, D., Rolbetzki, A., Boch, J., Kempf, B., Hoffmann, T., and Bremer, E. (2012) Genetic control of osmoadaptive glycine betaine synthesis in *Bacillus subtilis* through the choline-sensing and glycine betaine-responsive GbsR repressor. *J Bacteriol* **194**: 2703–2714.

Nguyen, M.T., and Götz, F. (2016) Lipoproteins of Gram-positive bacteria: key players in the immune response and virulence. *Microbiol Mol Biol Rev* **80**: 891–903.

Nicolas, P., Mäder, U., Dervyn, E., Rochat, T., Leduc, A., Pigeonneau, N., *et al*. (2012) Condition-dependent transcriptome reveals high-level regulatory architecture in *Bacillus subtilis*. *Science* **335**: 1103–1106.

Oh, B.H., Kang, C.H., De Bondt, H., Kim, S.H., Nikaido, K., Joshi, A.K., and Ames, G.F. (1994) The bacterial periplasmic histidine-binding protein. Structure/function analysis of the ligand-binding site and comparison with related proteins. *J Biol Chem* **269**: 4135–4143.

Oldham, M.L., and Chen, J. (2011) Crystal structure of the maltose transporter in a pretranslocation intermediate state. *Science* **332**: 1202–1205.

Oldham, M.L., Chen, S., and Chen, J. (2013) Structural basis for substrate specificity in the *Escherichia coli* maltose transport system. *Proc Natl Acad Sci U S A* **110**: 18132–18137.

Oldham, M.L., Davidson, A.L., and Chen, J. (2008) Structural insights into ABC transporter mechanism. *Curr Opin Struct Biol* **18**: 726–733.
Oldham, M.L., Khare, D., Quiocho, F.A., Davidson, A.L., and Chen, J. (2007) Crystal structure of a catalytic intermediate of the maltose transporter. *Nature* **450**: 515–521.
Orelle, C., Alvarez, F.J., Oldham, M.L., Orelle, A., Wiley, T.E., Chen, J., and Davidson, A.L. (2010) Dynamics of alpha-helical subdomain rotation in the intact maltose ATP-binding cassette transporter. *Proc Natl Acad Sci U S A* **107**: 20293–20298.
Orelle, C., Ayvaz, T., Everly, R.M., Klug, C.S., and Davidson, A.L. (2008) Both maltose-binding protein and ATP are required for nucleotide-binding domain closure in the intact maltose ABC transporter. *Proc Natl Acad Sci U S A* **105**: 12837–12842.
Oswald, C., Holland, I.B., and Schmitt, L. (2006) The motor domains of ABC-transporters. What can structures tell us? *Naunyn Schmiedebergs Arch Pharmacol* **372**: 385–399.
Oswald, C., Smits, S.H., Höing, M., Sohn-Bösser, L., Dupont, L., Le Rudulier, D., *et al.* (2008) Crystal structures of the choline/acetylcholine substrate-binding protein ChoX from *Sinorhizobium meliloti* in the liganded and unliganded-closed states. *J Biol Chem* **283**: 32848–32859.
Patzlaff, J.S., van der Heide, T., and Poolman, B. (2003) The ATP/substrate stoichiometry of the ATP-binding cassette (ABC) transporter OpuA. *J Biol Chem* **278**: 29546–29551.
Pittelkow, M., Tschapek, B., Smits, S.H., Schmitt, L., and Bremer, E. (2011) The crystal structure of the substrate-binding protein OpuBC from *Bacillus subtilis* in complex with choline. *J Mol Biol* **411**: 53–67.
Quentin, Y., Fichant, G., and Denizot, F. (1999) Inventory, assembly and analysis of *Bacillus subtilis* ABC transport systems. *J Mol Biol* **287**: 467–484.
Quiocho, F.A., and Ledvina, P.S. (1996) Atomic structure and specificity of bacterial periplasmic receptors for active transport and chemotaxis: variation of common themes. *Mol Microbiol* **20**: 17–25.
Ray, S.S., Bonanno, J.B., Chen, H., de Lencastre, H., Wu, S., Tomasz, A., and Burley, S.K. (2003) X-ray structure of an *M. jannaschii* DNA-binding protein: implications for antibiotic resistance in *S. aureus*. *Proteins* **50**: 170–173.
Rees, D.C., Johnson, E., and Lewinson, O. (2009) ABC transporters: the power to change. *Nat Rev Mol Cell Biol* **10**: 218–227.
Saier, M.H. Jr. (2000) A functional-phylogenetic classification system for transmembrane solute transporters. *Microbiol Mol Biol Rev* **64**: 354–411.
Scheepers, G.H., Lycklama, A.N.J.A., and Poolman, B. (2016) An updated structural classification of substrate-binding proteins. *FEBS Lett* **590**: 4393–4401.
Schöck, F., Gotsche, S., and Dahl, M.K. (1996) Vectors using the phospho-alpha-(1,1)-glucosidase-encoding gene *treA* of *Bacillus subtilis* as a reporter. *Gene* **170**: 77–80.
Shilton, B.H. (2008) The dynamics of the MBP-MalFGK(2) interaction: a prototype for binding protein dependent ABC-transporter systems. *Biochim Biophys Acta* **1778**: 1772–1780.
Shuman, H.A. (1982) Active transport of maltose in *Escherichia coli* K12. Role of the periplasmic maltose-binding protein and evidence for a substrate recognition site in the cytoplasmic membrane. *J Biol Chem* **257**: 5455–5461.
Smith, J.L., Goldberg, J.M., and Grossman, A.D. (2014) Complete genome sequences of *Bacillus subtilis* subsp. *subtilis* laboratory strains JH642 (AG174) and AG1839. *Genome Announc* **2**: e00663–14.
Smits, S.H., Höing, M., Lecher, J., Jebbar, M., Schmitt, L., and Bremer, E. (2008) The compatible-solute-binding protein OpuAC from *Bacillus subtilis*: ligand binding, site-directed mutagenesis, and crystallographic studies. *J Bacteriol* **190**: 5663–5671.
Steinke, A., Grau, S., Davidson, A., Hofmann, E., and Ehrmann, M. (2001) Characterization of transmembrane segments 3, 4, and 5 of MalF by mutational analysis. *J Bacteriol* **183**: 375–381.
Street, T.O., Bolen, D.W., and Rose, G.D. (2006) A molecular mechanism for osmolyte-induced protein stability. *Proc Natl Acad Sci U S A* **103**: 13997–14002.
Tam, R., and Saier, M.H. Jr. (1993) Structural, functional, and evolutionary relationships among extracellular solute-binding receptors of bacteria. *Microbiol Rev* **57**: 320–346.
van der Heide, T., and Poolman, B. (2002) ABC transporters: one, two or four extracytoplasmic substrate-binding sites? *EMBO Rep* **3**: 938–943.
von Blohn, C., Kempf, B., Kappes, R.M., and Bremer, E. (1997) Osmostress response in *Bacillus subtilis*: characterization of a proline uptake system (OpuE) regulated by high osmolarity and the alternative transcription factor sigma B. *Mol Microbiol* **25**: 175–187.
Warren, C. (2016) Do microbial osmolytes or extracellular depolymerization products accumulate as soil dries? *Soil Biol Biochem* **98**: 54–63.
Webb, B.A., Karl Compton, K., Castaneda Saldana, R., Arapov, T.D., Keith Ray, W., Helm, R.F., and Scharf, B.E. (2017) *Sinorhizobium meliloti* chemotaxis to quaternary ammonium compounds is mediated by the chemoreceptor McpX. *Mol Microbiol* **103**: 333–346.
Welsh, D.T. (2000) Ecological significance of compatible solute accumulation by micro-organisms: from single cells to global climate. *FEMS Microbiol Rev* **24**: 263–290.
Wilkinson, S.P., and Grove, A. (2006) Ligand-responsive transcriptional regulation by members of the MarR family of winged helix proteins. *Curr Issues Mol Biol* **8**: 51–62.
Winkelman, J.T., Bree, A.C., Bate, A.R., Eichenberger, P., Gourse, R.L., and Kearns, D.B. (2013) RemA is a DNA-binding protein that activates biofilm matrix gene expression in *Bacillus subtilis*. *Mol Microbiol* **88**: 984–997.
Wuttge, S., Bommer, M., Jager, F., Martins, B.M., Jacob, S., Licht, A., *et al.* (2012) Determinants of substrate specificity and biochemical properties of the sn-glycerol-3-phosphate ATP binding cassette transporter (UgpB-AEC2) of *Escherichia coli*. *Mol Microbiol* **86**: 908–920.
Yu, J., Ge, J., Heuveling, J., Schneider, E., and Yang, M. (2015) Structural basis for substrate specificity of an amino acid ABC transporter. *Proc Natl Acad Sci U S A* **112**: 5243–5248.

Supporting information

Additional supporting information may be found in the online version of this article at the publisher's web-site.